Journal of Materials Chemistry B

ROYAL SOCIETY OF CHEMISTRY

REVIEW

View Article Online
View Journal | View Issue

Check for updates

Cite this: J. Mater. Chem. B, 2020, 8, 7571

Three-dimensional scaffold-free microtissues engineered for cardiac repair

Alejandra Patino-Guerrero,[a] Jaimeson Veldhuizen,[a] Wuqiang Zhu,[b] Raymond Q. Migrino[cd] and Mehdi Nikkhah *[ae]

Cardiovascular diseases, including myocardial infarction (MI), persist as the leading cause of mortality and morbidity worldwide. The limited regenerative capacity of the myocardium presents significant challenges specifically for the treatment of MI and, subsequently, heart failure (HF). Traditional therapeutic approaches mainly rely on limiting the induced damage or the stress on the remaining viable myocardium through pharmacological regulation of remodeling mechanisms, rather than replacement or regeneration of the injured tissue. The emerging alternative regenerative medicine-based approaches have focused on restoring the damaged myocardial tissue with newly engineered functional and bioinspired tissue units. Cardiac regenerative medicine approaches can be broadly categorized into three groups: cell-based therapies, scaffold-based cardiac tissue engineering, and scaffold-free cardiac tissue engineering. Despite significant advancements, however, the clinical translation of these approaches has been critically hindered by two key obstacles for successful structural and functional replacement of the damaged myocardium, namely: poor engraftment of engineered tissue into the damaged cardiac muscle and weak electromechanical coupling of transplanted cells with the native tissue. To that end, the integration of micro- and nanoscale technologies along with recent advancements in stem cell technologies have opened new avenues for engineering of structurally mature and highly functional scaffold-based (SB-CMTs) and scaffold-free cardiac microtissues (SF-CMTs) with enhanced cellular organization and electromechanical coupling for the treatment of MI and HF. In this review article, we will present the state-of-the-art approaches and recent advancements in the engineering of SF-CMTs for myocardial repair.

Received 19th June 2020,
Accepted 21st July 2020

DOI: 10.1039/d0tb01528h

rsc.li/materials-b

Published on 21 July 2020. Downloaded by ASU Library on 2/2/2021 12:58:01 AM.

[a] School of Biological and Health Systems Engineering, Arizona State University, Tempe, AZ, USA. E-mail: mnikkhah@asu.edu
[b] Department of Cardiovascular Diseases, Physiology and Biomedical Engineering, Mayo Clinic, Scottsdale, AZ, USA
[c] Phoenix Veterans Affairs Health Care System, Phoenix, AZ, USA
[d] University of Arizona College of Medicine, Phoenix, AZ, USA
[e] Biodesign Virginia G. Piper Center for Personalized Diagnostics, Arizona State University, Tempe, AZ, USA

Alejandra Patino-Guerrero

Alex earned her BS degree in Bioengineering from the Autonomous University of Baja California. Currently she is on her third year as a PhD student in the Biomedical Engineering program of the Arizona State University. Her research interests are focused on the integration of biology and engineering towards cardiac regenerative medicine and the development of innovative engineered tissues.

Mehdi Nikkhah

Mehdi Nikkhah is currently an Associate Professor of Bioengineering at the School of Biological and Health Systems Engineering (SBHSE), Arizona State University. He completed his postdoctoral fellowship training at Harvard Medical School and PhD degree at Virginia Tech. His research interest is focused on the integration of micro- and nanoscale technologies, innovative biomaterials, and biology to better understand the mechanisms of human disease progression and to develop regenerative medicine strategies to treat organ/tissue failure.

Published on 21 July 2020. Downloaded by ASU Library on 2/2/2021 12:58:01 AM.

1. Introduction

Around 6.5 million people in the United States experienced heart failure (HF) in 2016, with several thousand patients on a waiting list to receive a heart transplant.[1] It is estimated that by 2030 more than 8 million will present with this condition.[2] Cardiovascular diseases (CVDs), including myocardial infarction (MI), remain a leading cause of mortality and morbidity worldwide, accounting for over 30% of all human deaths.[3] MI leads to loss of cardiomyocytes (CMs), which have limited regenerative capacity, as well as to decreased contractility, adverse remodeling of the myocardium, and ultimately HF.[4] While age-adjusted CVD-related deaths have declined by about two-thirds in industrialized nations[5] and the rate of acute hospitalization for HF in the US has declined from 2006 to 2014, the burden of HF remains considerable with 84 000 deaths primarily due to HF and total estimated cost of $11 billion in 2014.[6]

Cardiac damage can result from various insults such as ischemic (*i.e.*, MI), infectious (myocarditis), toxic (post-chemotherapy), infiltrative (amyloidosis), valvular (regurgitant or stenotic lesions) or other causes.[7,8] Despite the variety of underlying causes, significant loss of viable myocardium leads to shared pathogenetic mechanisms involving neurohormonal dysregulation, hemodynamic overload, cardiac remodeling, abnormal calcium cycling, and extracellular matrix (ECM) dysfunction.[9,10] The healthy myocardium presents aligned fibers (Fig. 1A(i) and B(i)); however, after MI, the heart undergoes an inflammatory stage, characterized by the presence of immune cell infiltration and the formation of granulation tissue (Fig. 1A(ii) and B(ii)). Later, the resolution of the inflammatory stage leads to collagen deposition by myofibroblasts, resulting in thin hypocellular fibrotic tissue (Fig. 1A(iii) and B(iii)).[11,12] The loss of viable CMs, in addition to the subsequent formation of fibrotic/scar tissue, leads to critical complications after MI,[13] such as the loss of mechanical contraction, which is often measured through the left ventricle (LV) ejection fraction (LVEF).[14] Due to the extremely low renewal rate of CMs in the heart,[15] CMs are not able to repopulate the damaged tissue in a timely manner to restore the normal function of the heart, leading to persistence and expansion of the non-compliant damaged tissue.[16] A small population of multipotent stem cells, referred to as cardiac progenitor cells (CPCs), has been recently discovered to reside in the heart. However, the role of CPCs in the functional regeneration of the myocardium is still not clear and remains a controversial subject. It is believed that the primary function of CPCs lies in paracrine signaling rather than proliferation and repopulation of damaged cardiac tissue.[17–19]

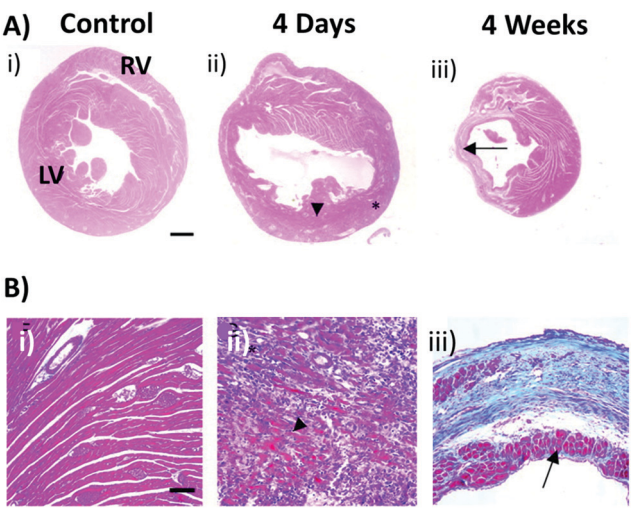

Fig. 1 Stages of remodeling of the heart post-MI (murine). (A) Hematoxylin and Eosin (H&E) staining of (i) healthy myocardium, (ii) 4-day infarcted heart showing necrosis encapsulation (arrow head) and granulation tissue (*), and (iii) 4-week infarcted heart showing thinning of the ventricular wall. (Scale bar 0.5 mm) (B) Masson trichrome staining of (i) healthy myocardium, (ii) 4-day infarcted heart (arrow head: necrosis), and (iii) 4-week infarcted heart showing collagen deposition (blue). (Scale bar: 100 μm.) Adapted with permission from the American Society for Investigative Pathology [*Am. J. Pathol.*], (Virag *et al.*) Copyright © (2003), from ref. 11.

Current pharmacologic therapy approaches rely on relieving the hemodynamic burden (afterload and preload reduction) to reduce stress on the remaining functional myocardium and modulating neurohormonal pathways that are triggered to compensate for reduced myocardial function.[20] Three classes of drugs, including angiotensin-converting enzyme inhibitors/angiotensin II receptor blockers, aldosterone antagonists, and β-adrenergic blockers, as well as the implantation of internal cardioverter defibrillation and cardiac resynchronization therapy, have been shown to improve survival in patients with HF with reduced ejection fraction.[10] However, these approaches, while improving the function of the remaining viable myocardium and slowing adverse myocardial remodeling, do not replace the damaged myocardium. If pharmacologic therapy fails, heart transplantation or implantation of mechanical left ventricular assist device (LVAD) are treatment options of last resort. However, these approaches are still limited by an inadequate number of organ donors and potential complications derived from surgical procedures.[21] For instance, it has been demonstrated that LVAD promotes pathophysiological changes in the ECM of the myocardium by increasing collagen cross-linking and tissue stiffness (*i.e.*, fibrosis), leading to inadequate contractility.[22] Additionally, the introduction of allograft organs elicits an immunologic response that can lead to acute rejection of the transplanted heart. To reduce this response, heart-transplanted patients undergo immunosuppression therapies; however, these therapies often lead to chronic side-effects.[23]

The field of cardiac regenerative medicine has surged in the past decade as a potentially powerful alternative approach, to the current pharmacological and surgical interventions, for treatment of MI and HF. The focus of cardiac regenerative medicine, and the strategies derived from it, is the repair and regeneration of the damaged myocardium upon MI to regain heart function and avoid the side effects and complications of traditional therapies. Despite significant advancements, there are still numerous challenges facing cardiac regenerative medicine such as notable loss of implanted cells, poor cellular survival and coupling, and lack of integration/engraftment of the engineered tissues with the host myocardium. To that end,

 This journal is © The Royal Society of Chemistry 2020

Published on 21 July 2020. Downloaded by ASU Library on 2/2/2021 12:58:01 AM.

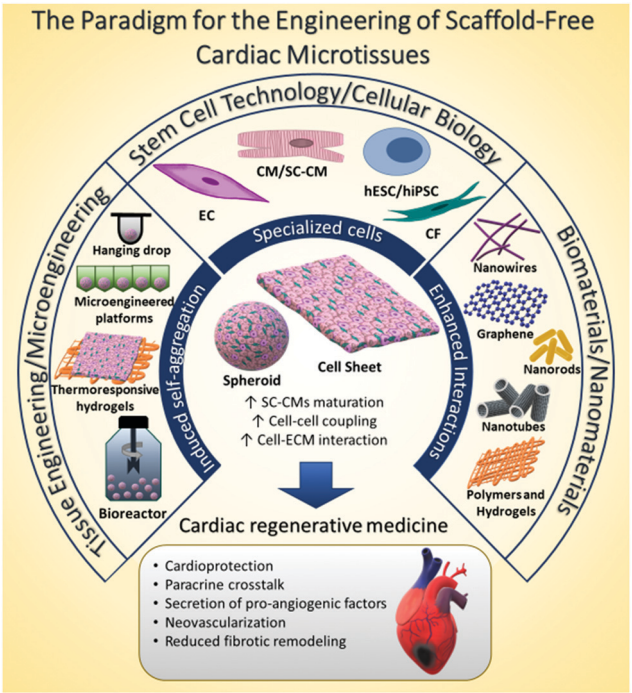

Fig. 2 The paradigm for engineering of scaffold-free cardiac microtissues (SF-CMTs). The development and fabrication of SF-CMTs based on a multi-disciplinary approach, benefited from advancements in differentiation and characterization of stem cells as well as technological advancements in tissue engineering, micro- and nanoscale fabrication techniques, use of nanomaterials, *etc.* The use of SF-CMTs have demonstrated to be a promising approach for treatment of MI by providing cardioprotective effects, such as the induction of neovascularization and paracrine crosstalk. ↑ indicates increase or enhancement. Abbreviations: hESC: human embryonic stem cells, hiPSC: human induced pluripotent stem cells, CMs: cardiomyocytes, SC-CMs: stem cell-derived cardiomyocytes, CFs: cardiac fibroblasts, ECs: endothelial cells.

innovative regenerative medicine approaches are still emerging based on the advancements of stem cell bioengineering, and micro- and nanoscale technologies, to address these critical shortcomings (Fig. 2). In this review article, we broadly highlight different approaches in cardiac regenerative medicine, discuss their advantages and shortcomings, and present how the challenges of traditional and conventional therapies could be overcome. We will then specifically explore different methods and materials used for the development of scaffold-free cardiac microtissues (SF-CMTs) and discuss their promising potential for myocardial repair and regeneration. We will further review the integration of nanomaterials with SF-CMTs, present commonly used nanomaterials, and evaluate specific study cases. Lastly, we will address the remaining challenges of engineering and application of SF-CMTs and provide our prospective for future advancements in this field.

2. Cell-based cardiac therapy

Recent therapeutic approaches for treatment of MI and chronic HF are based on recellularizing the myocardium and eliciting the repairment and regeneration of the injured tissue.[24] The most straightforward techniques are based on bolus injection of either dissociated stem/progenitor cells or terminally differentiated cells through various delivery routes such as intracoronary and intramyocardial injections.[25] Cell-based cardiac therapy aims to elicit the self-regeneration of the heart by introducing paracrine signaling cues and repopulating the damaged tissue with new healthy cells in order to improve the overall function and structural integrity of the myocardium.[26] The selection of target cells from different sources is based on two main parameters: first, the potential for the cells to recellularize the damaged myocardium based on their proliferative and differentiation capacity; and second, their availability and abundance for harvesting and expansion *in vitro*.[27] To date, stem and progenitor cells have been widely utilized for cell-based cardiac therapies due to their self-renewal capabilities and their potential to differentiate into cardiac lineages. Different sources have been used to obtain these cells with varying degrees of success.[28] Some of the most widely utilized cells for cardiac regeneration are mesenchymal stem cells (MSCs), CPCs, embryonic stem cells (ESCs), and more recently, induced pluripotent stem cells (iPSCs). A comprehensive review of stem cell-based cardiac therapy for the treatment of MI and HF has been completed elsewhere.[29] Herein, we briefly present representative studies of relevance for the field.

Adipose tissue has been identified as a viable source of MSCs due to its accessibility and ease of harvesting.[30,31] Additionally, bone marrow (BM) has also been proposed as a suitable source of autograft MSCs for cell-based cardiac therapy. For instance, the therapeutic effect of these cells was evaluated in a study involving sixty-nine randomized patients with acute MI who received autologous intracoronary transplantation of BM-MSCs or saline solution.[32] The investigators demonstrated that, three months after injection, the implanted BM-MSCs were viable and engrafted with the host myocardium. Cardiac function was improved in the group that received the BM-MSCs, measured by increased ejection fraction and decreased perfusion defects. However, the final differentiation stage of the implanted cells and the detailed mechanism of the improvement of cardiac function were not elucidated in this study. Therefore, more in-depth mechanistic studies are necessary to understand better the role of these cells in improved clinical outcomes.

Cardiac tissue has also been proposed as a source for resident cardiac stem cells. For instance, CADUCEUS was a phase I clinical trial involving the delivery of autologous CPCs through intracoronary infusion after MI.[33] CPCs were extracted from an endomyocardial biopsy and injected into the myocardium 1.5–3 months after MI. The patients were observed for six months post-procedure, and no functional improvements were noted upon treatment. However, a significant reduction in scar mass, as well as a significant increase in viable heart tissue, were observed in comparison to the control group. Despite the significance of these studies, sourcing of stem cells from primary adult tissues presents technical challenges,[34] such as the harvesting of sufficient cells and the preparation of the cells prior to their implantation.

Published on 21 July 2020. Downloaded by ASU Library on 2/2/2021 12:58:01 AM.

Pluripotent stem cells have also been proposed as an alternative and powerful source of cells for cardiac therapy, with extensive studies demonstrating the great potential of these cells for organ regeneration in clinical trials.[35,36] Protocols for *in vitro* differentiation of ESCs towards CMs have been developed[37] and optimized,[38] and have enabled the use of human ESCs-derived CMs (hESC-CMs) for myocardial replacement therapy. For instance, in a recent work, the feasibility for using hESC-CMs in cardiac therapy was tested in non-human primate models of MI.[39] hESC-CMs were delivered intramyocardially in the infarct and border zones. The explanted hearts that received the cell treatment showed extensive remuscularization, denoted by the presence of human cells in the infarct zone. Moreover, there was evidence of the formation of nascent intercalated disks, suggesting host–graft electromechanical coupling. However, the specimens that received cellular transplantation showed arrhythmias, most likely due to the immature state of the hESC-CMs. A similar study from a different group found that, due to the remuscularization of the myocardium injected by hESC-CMs, the mechanical function of the heart was improved (increased LVEF).[40] Overall, hESC-CMs are a promising alternative for cardiac cell-based therapies; however, more understanding of the mechanisms leading to arrhythmia is needed. In addition, ethical issues associated with the use of hESCs have limited the potential of these cells for cardiac therapy.

The successful reprogramming of human somatic cells into induced pluripotent stem cells (hiPSCs) in 2007[41,42] opened a unique window of opportunity for cell-based regenerative therapies. The possibility of obtaining hiPSCs without the ethical and technical challenges of sourcing them has led to extensive investigations of their potential, specifically for heart regeneration. There have been several advancements in directed differentiation protocols of hiPSC-CMs *in vitro* since the establishment of the first protocol in 2009.[43] Since then, several methods have been tested and optimized to increase the production yield of CMs and other cardiac-associated cells without the technical and ethical issues as well as accessibility limitations associated with the use of ESC-CMs. Differentiation of hiPSCs toward cardiac lineage often requires a purification stage to increase the yield of produced CMs. This purification step has been particularly critical, as it is well accepted that differentiation protocols could also produce other cell types such as fibroblasts or endothelial cells (ECs).[44] The potential of hiPSC-CMs for cardiac repair has started to be explored in a recent reported clinical trial. This study involved direct injection of allogenic hiPSC-CMs in the myocardium of patients with severe LV disfunction and MI history, at the same time of a coronary artery bypass grafting surgery (ClinicalTrials.gov Identifier: NCT03763136: Treating Heart Failure With hPSC-CMs (HEAL-CHF)).[45] Despite promising efforts, the study is still ongoing, and no peer-reviewed results have been published to the date. To that end, more studies are needed in order to evaluate the efficacy of hiPSC-CMs in cardiac therapy.

2.1. Challenges of cell-based cardiac therapy

As discussed earlier, injection of dissociated cells in preclinical studies and clinical trials has demonstrated modest improvement in overall cardiac function, attributed mainly to the paracrine communication of the implanted cells with the native host tissue. For instance, the secretion of angiogenic factors and extracellular vesicles within the native tissue have shown to induce neovascularization within the implanted zones.[46] To that end, despite significant advancements, there are still several setbacks regarding cell-based cardiac therapy approaches. First, there is no consensus over the optimal cell type or delivery method to be used since the outcome could be widely influenced by the cell type, the stage of the MI, *etc.*[47] Additionally, there is a lack of control over the differentiation fate of the stem/progenitor cells upon implantation, as the harsh microenvironment within the infarcted myocardium appears not to favor CM fate[27] (*e.g.*, endothelial fate is favored in the native myocardium).

Furthermore, engraftment in non-target organs has been reported by several authors.[48] Therefore, more thorough screenings are necessary to discard teratogenic risks.[49] Additionally, one of the main differences between clinical trials and preclinical studies is the time elapsed between MI and cell injection. In general, for animal models, the extraction, purification, and expansion or differentiation of stem cells are performed before induction of MI, where the cells are injected within a timeframe of a few hours. However, in the case of human patients, it can take several weeks from the extraction of the primary tissue to the final expansion of stem cells, where it has been suggested that the time immediately after MI might be a critical window of opportunity to obtain an efficient outcome.[32,50] It is also well accepted that the recellularization of damaged tissue is dependent on the extent of the scar or fibrotic area. Yet, there is no consensus on the number of cells necessary for injection. In clinical settings, this proves to be more challenging to optimize and standardize since each case presents different localization and extent of damage, contrary to the preclinical models, where the extent and type of cardiac injury are precisely controlled following well-defined protocols. Ultimately, the issue of controlling stem cell fate *in vivo* has led researchers to differentiate stem cells into cardiac lineage *in vitro*, then evaluate the efficacy of implanted stem cell-derived cells for their therapeutic potential. The use of autograft hiPSCs or hiPSC-derived cells for regenerative cardiac therapy may potentially reduce the risk of incompatibility and immune reaction upon cellular or tissue implantation as compared to other cells.[51] However, it is known that one of the main disadvantages of using either hiPSC- or hESC-CMs for regenerative medicine is their relatively immature phenotype, resembling more a fetal state than an adult phenotype,[52] characterized by poor development of sarcomeric apparatus,[53] smaller size than adult CMs, and inadequate electrophysiological activity (Ca^{2+} handling and action potential).[52] The immature profile of hiPSC- or hESC-CMs may also lead to several complications after implantation due to the failure of engraftment and synchronization with the native tissue. In addition, there have been some reports discussing the potential risk of tumor formation upon injection of stem cell-derived cells.[54] To address these limitations, tissue engineering approaches have been widely investigated for the development of mature cellular aggregates or tissue surrogates for repair and regeneration of damaged myocardium. In the next section, we discuss tissue engineering

 This journal is © The Royal Society of Chemistry 2020

Published on 21 July 2020. Downloaded by ASU Library on 2/2/2021 12:58:01 AM.

technologies, highlighting the advantages and disadvantages of each approach, with a particular focus on scaffold-free cardiac tissue engineering strategies.

3. Microscale tissue engineering for cardiac regeneration

Tissue engineering approaches have emerged in the past decades to develop *in vitro* functional cellular structures that can be readily integrated into the host myocardium as potentially powerful alternatives strategy for the treatment of MI.[55] While early attempts focused on engineering of macroscale tissue constructs, the advancements in microscale technologies (*i.e.*, microengineering) in the past few years have provided a unique ability to develop biomimetic tissue models with native-like properties and cellular/ECM organization for regenerative medicine and disease modeling applications (*e.g.* cancer).[56–62] The use of microengineering technologies for cardiac disease modeling and drug screening, in recent years, has been demonstrated and discussed extensively.[56,63–66] The scope of the current manuscript is to provide a review on microscale engineered cardiac tissues or, in other words, engineering of "*cardiac microtissues*" (CMTs), for myocardial repair therapy. A microtissue can be broadly defined as an engineered three-dimensional (3D) biological structure within the micrometer range, which is formed by the functional aggregation of one or more cell types. Assembly of microtissues may or may not be supported by natural or synthetic biomaterials, such as ECM proteins and hydrogels.[67] Engineered microtissues can be generally categorized into two different groups: scaffold-based and scaffold-free microtissues. The 3D environment within the engineered microtissues provides a natural niche for cellular assembly with enhanced cell–cell interactions, physiologically relevant autocrine and paracrine signaling, as well as improved function that mimic the *in vivo* conditions.[68] A key advantage in utilizing microscale technologies for engineering cardiac tissues is the induction of precise cellular organization and architecture, often in conjunction with modulated electromechanical cues.[69] Particularly, in the native heart, the structural anisotropy and architecture of the myocardium are as critical as the cellular and ECM composition of the tissue, which modulate physiologic tissue-level homeostasis and function. This 3D cellular organization is paramount to produce synchronized and unidirectional contractions. Conversely, cell misalignment has been linked to disruption of tissue homeostasis and emergence of several cardiovascular diseases.[70,71] To that end, tissue engineering, and specifically microscale tissue engineering approaches, provide more robust methods to precisely modulate cellular and tissue-level structure and function to address limitations of cell-based cardiac therapies.

3.1. Optimized cell culture for engineering of cardiac microtissues (CMTs)

Although numerous cell types have been used to engineer CMTs, not all cells are suitable for the use in cardiac regeneration to achieve the desired function and structural outcomes. The use of donor primary stem cells, such as those extracted from BM, adipose tissue, or cardiac muscle, represents a significant challenge due to the need for extensive *in vitro* expansion procedures. The use of ESCs also raises ethical concerns.[72] To that end, in recent years, there has been significant attention toward the use of hiPSCs in cardiovascular regeneration, similar to cell-based cardiac therapy. Different strategies thus far have been proposed to improve the maturation state of hiPSC-CMs for their use in engineering of functional CMTs. These approaches have aimed to mimic the microenvironment of the heart by introducing specific cues to the cell culture, which have been thoroughly reviewed by several authors.[73–76] Evaluation of the maturation state of hiPSC-CMs is not trivial, and different markers have been utilized to determine their maturity level. Functional maturation has been traditionally defined by three principal factors: (a) structural features, as measured by increased cell size, elongated morphology,[77] organization of sarcomeric structures,[78] and upregulation of cellular ultrastructure-related genes (MYH7, GJA1, TNNI3, AKAP6, GJA5, JPH2);[79] (b) enhanced electrophysiological properties, such as increased action potential amplitude, lower resting membrane potential and increased conduction velocity,[73] and Ca^{2+} handling (increased calcium release and reuptake rates)[77] along with upregulation of Ca^{2+} handling genes (CAV3, BIN1, ATP2A2, RYR2, ITPR3);[79] and finally (c) increased mechanical function, measured through higher contraction force[80] when compared to fetal-state CMs along with regulation of contractile function-related genes, such as upregulation of the ones encoding for cTnT, αMHC, CASQ2, SERCA2,[81] ITPR3, KCNH2 and downregulation of HCN4.[79] At the molecular level, metabolic changes and regulation of genetic programs have also been among the critical markers of hiPSC-CM maturation. For example, a shift from glycolytic to oxidative metabolism is a marker for metabolic maturation, which indicates an increase in the oxidative capacity of the mitochondria.[82,83] This better resembles the energy sourcing and utilization of CMs in the native myocardium after birth. Other metabolic markers, including the enrichment of phospholipid metabolism and pantothenate and coenzyme A metabolism, have been also identified as indicators of maturation.[84]

It has been reported that the presence of a 3D microenvironment within engineered CMTs can notably improve the structural and functional maturation of hiPSC-CMs. For example, in a recent study, Correia *et al.* characterized and compared the metabolic function of hiPSC-CMs cultured in 3D cell aggregates compared to 2D cell culture.[83] hiPSC-CMs cultured within the 3D environment shifted towards an oxidative metabolism, whereas 2D cultured cells exhibited glycolytic metabolism, which is less energy-efficient and is associated with a more immature phenotype. Electrophysiological properties, as defined through extended action potential duration, were also improved in the 3D cell aggregates. While the complete mechanism of metabolic regulation has not been well understood yet, it was suggested that 3D cell culture favors the paracrine, autocrine, and endocrine communication. Therefore, it was proposed that

Published on 21 July 2020. Downloaded by ASU Library on 2/2/2021 12:58:01 AM.

maturation of hiPSC-CMs was driven by downregulation of the PI3K/AKT/insulin pathway and upregulation of genes involved in fatty acid metabolism. A combination of maturation-inducing techniques has been another viable strategy to enhance the maturation of hiPSC-CMs, similar to the native myocardium. A prominent example is the biowire platform created by Nunes *et al.*, which combined the use of two different scaffolds, namely a surgical suture and type I collagen matrix, along with electrical stimulation to improve the functional maturation of hiPSC-CMs.[85] Using this platform, the electrophysiological features of the hiPSC-CMs improved, resembling more closely the characteristics of the native adult CMs.

Overall, it is paramount to utilize strategies to induce a more mature phenotype in hiPSC-CMs within engineered CMTs to enable safer and more efficient engraftment as well as synchronization upon implantation or injection into the native myocardium.

3.2. Engineering scaffold-based cardiac microtissues (SB-CMTs)

Engineering of SB-CMTs requires at least two primary components: first, a biomaterial matrix that serves as scaffolding support and offers a 3D ECM-like structure within the engineered tissues, and second, cells of interest to populate within the 3D environment of the matrix. The use of scaffolding biomaterials for the creation of engineered CMTs serves several purposes. Primarily, the scaffold matrix could mimic the native tissue ECM, offering mechanical support for the cells to undergo morphogenesis and assemble in a 3D architecture. Integrated architectural and topographical cues can also be introduced within the engineered scaffolds.[86–88] For example, anisotropy in engineered CMTs enables enhanced CMs alignment, contractile stress generation, and improved electrophysiological functions.[89] It has been also demonstrated that scaffold stiffness plays a crucial role in the biological function and metabolism of encapsulated cells in general[90] and particularly CMs. Independent studies have shown that, when encapsulating CMs or CPCs, the amplitude of contraction and expression of specific genes (*e.g.*, VWF and CNN1 in case of CPCs) can be modulated by changes in the stiffness of the scaffolding matrix.[91–94] Biochemical signaling cues have also been introduced to SB-CMTs through modification of the chemical moieties and composition of scaffolds[95,96] or the incorporation of growth factors.[97] Recently, it was demonstrated that cellular constructs fabricated with varying types of cells, for instance hESC-derived CMs in coculture with hESC-derived epicardial cells, embedded in collagen matrices, present a more mature state and improved capacity for remuscularization of infarcted myocardium.[98] Additional components, such as vascular-like structures,[99,100] can also be integrated within the SB-CMTs through different fabrication strategies (*e.g.*, bioprinting, micropatterning).[58] The use of scaffolding biomaterials also enables precise manipulation of electrical or mechanical cues within the 3D tissue environment through exogenous signals, such as conductive nanomaterials or cyclic mechanical stretch, for improved cellular- and tissue-level functions.[85,99,101–106]

To date, several natural and synthetic materials have been identified as biocompatible candidates for cardiac tissue engineering.[88] For example, fibrin[107] and collagen[108] have been among the natural-derived hydrogels used for the development of SB-CMTs construction. Some of the frequently used synthetic polymers for cardiovascular tissue engineering include poly(*N*-isopropylacrylamide) (poly(NIPAAm)),[109–112] polylactic acid (PLA), polyglycolic acid (PGA), poly(glycerol sebacate) (PGS), among others.[113] There has also been extensive work in the development of composite,[114] electrospun,[115,116] and nano-engineered[103,117] scaffolds with well-tuned mechanical and electrical properties to engineer highly functional SB-CMTs. While there have been numerous review articles providing excellent overviews on the types and characteristics of scaffolding biomaterials for cardiac tissue engineering, the subject of SB-CMTs is out of the scope of the present review article, and the readers are referred to earlier works.[118]

3.2.1. Challenges of scaffold-based cardiac tissue engineering.

The use of scaffolding biomaterials in cardiac tissue engineering offers a robust strategy for cellular delivery and engraftment of the engineered tissue with the host myocardium. Moreover, it has been observed in preclinical trials that the implantation of SB-CMTs (*i.e.*, cardiac patches) can have paracrine effects in the myocardium, that could lead to angiogenesis and reduced infarct size.[119] However, the delivery method of SB-CMTs to the target site within the host myocardium is subject to factors such as the size and geometry of the engineered tissue. Generally, SB-CMTs are constructed in the form of patches or sheets and are implanted in the heart *via* thoracotomy or thoracoscopy surgery, which are highly invasive routes. Moreover, there is no agreement on the optimal location for the patch implantation.[120] Furthermore, engineering of SB-CMTs that are compatible with the host myocardium and its complex microenvironment is not a trivial task. It is well known that the stiffness of the myocardium can change according to the developmental stage, age, and stage of the cardiac disease of the patient. While immature hiPSC-CMs adapt better to scaffolds resembling the neonatal stiffness of the heart, the performance of SB-CMTs may benefit from a well-tuned stiffness similar to the one of the adult heart.[121] Cell behavior is also heavily influenced by the mechanical properties (stiffness, swelling, cross-link density) of the scaffolding matrix, causing the cells to behave differently as compared to the native tissue.[122–124] Degradation of scaffolding biomaterials may also pose another challenge in the implantation of SB-CMTs. For instance, a delicate balance between degradation rate and cellular interconnection and deposition of new ECM needs to be achieved. If the scaffold degrades too quickly, the delivered cells will not have the opportunity to form sufficient cell-to-cell and cell-to-ECM interactions to support their engraftment. On the other hand, if the scaffold does not degrade fast enough, it can elicit a foreign body reaction and fibrotic encapsulation.[125] In either case, there is a need for better optimization of a suitable degradation rate of the matrix. Also, it has been reported that ECM-derived scaffolds may exhibit immunogenic activity[126] and elicit immune response (chronic inflammation, implant rejection) within the native tissue upon implantation. To that

 This journal is © The Royal Society of Chemistry 2020

Published on 21 July 2020. Downloaded by ASU Library on 2/2/2021 12:58:01 AM.

end, the clearance pathways and potential toxicity of the degradation byproducts need to be well studied prior to proceeding clinical trials.

4. Scaffold-free cardiac tissue engineering

With the advancements in innovative tissue engineering strategies aided by micro- and nanoscale technologies, engineering of scaffold-free cardiac microtissues (SF-CMTs) have been proposed as a potentially attractive alternative to bridge the existing gap between cell-based cardiac therapy and scaffold-based tissue engineering approaches. Engineering of SF-CMTs offers the robustness and enhanced organization of SB-CMTs with the potential for less-invasive delivery methods, similar to cell-based cardiac therapies,[127] without the introduction of exogenous biomaterials. SF-CMTs can range from basic self-assembled spheroid cell aggregates, formed exclusively from primary CMs or stem cell-derived cells[128,129] to more complex organoid structures composed of different cell types, such as CMs, cardiac fibroblasts (CFs), ECs, and even CPCs.[130–132] In addition, through the incorporation of microengineering technologies, it has been possible to precisely control the architecture, cellular organization, and size/geometry of SF-CMTs. In the following sections, we discuss the relevant properties and features of SF-CMTs as well as the main fabrication strategies and highlight key study cases in the engineering of SF-CMTs for cardiac repair.

4.1. Size and geometry

It is well accepted that a gradient of oxygen and nutrients is formed within engineered tissue constructs due to the lack of proper vascularization and packing cellular density.[133] Induction of hypoxic or necrotic cores is desirable for disease modeling (*i.e.*, MI, ischemia, *etc.*) and drug screening.[134] However, in the case of regenerative medicine, microtissues, specifically SF-CMTs, must be engineered carefully to maintain cell viability to allow for engraftment and survival after implantation within the host myocardium. Different mathematical models have been developed in order to predict and optimize the best size-to-diffusion limit ratio of microtissues and organoids.[135–137] Still, that ratio might vary according to the metabolic demands of the various cell types used for the fabrication of SF-CMTs. For instance, it has been reported that hiPSC-CMs cultured in 3D microenvironments have a higher metabolic rate than in 2D cultures.[138] As a consequence, higher concentrations of oxygen and nutrients, as well as a higher waste product removal rate are required.[83,139] In order to elucidate the optimal size for enhanced cell-to-cell interactions and diffusion limitations, Tan *et al.* constructed hiPSC-CMs spheroids of varying sizes and measured oxygen consumption rates, and their metabolic and electrophysiological activity.[138] It was demonstrated that spheroids with a radius of $\sim$150 μm (about 3000 cells per spheroid) presented the optimal metabolic activity while maximizing the benefits from the 3D microenvironment created within the microtissue.

The introduction of ECs has been proposed as an alternative to overcome the diffusion restriction in order to produce SF-CMTs with physiologically relevant sizes. The goal is to form vasculature-like structures within the microtissues that can carry oxygen and nutrients to the inner-most areas, allowing for the formation of larger, healthier scaffold-free tissues.[140–142] In a recent study, Pitaktong *et al.* fabricated spherical SF-CMTs with hiPSC-CMs, CFs, and hiPSC-derived early vascular cells (which can differentiate into ECs or pericytes) in a ratio of 7 : 1.5 : 1.5 respectively.[143] Spheroids with diameters up to 500 μm were viable and exhibited organized vasculature-like structures. In addition to enhanced cell organization and primitive microvasculature, it was believed that the presence of ECs and CFs increased the resistance of the CMs to hypoxic conditions *via* paracrine signaling. Similarly, Beauchamp *et al.* created scaffold-free 3D cocultures of hiPSC-CMs and primary embryonic CFs[144] (Fig. 3A(i and ii)) to elucidate the influence and role of CFs in the formation of SF-CMTs. It was found that the presence of CFs in the 3D coculture influenced the morphology (elongated) and maturation stage (higher expression of cTnI) of the hiPSC-CMs, making them more similar to adult CMs. Noguchi *et al.* also proposed the use of ECs and fibroblasts to create vascularized scaffold-free cardiac patches.[140] For this purpose, they used neonatal rat CMs, human ECs, and human dermal fibroblasts to create spheroids (Fig. 3B(i)). Vasculature formation was observed within the spheroids, which were further assembled to form cardiac patches of up to 10 mm of diameter (Fig. 3B(ii–vi)). It was reported that the ratio of CMs : ECs : CFs affects the functionality of SF-CMTs, with an optimal cellular ratio of 7 : 1.5 : 1.5 (CMs : ECs : CFs). Fractional shortening (FS) was directly proportional to the percentage of CMs in the spheroid, with a higher FS in pure CM-derived SF-CMTs when compared to multicellular SF-CMTs. However, multicellular constructs displayed enhanced cellular organization and functioning microvascular structures. When implanted in mouse hearts, the optimized multicellular SF-CMTs successfully adhered to the native LV with the evidence of blood flow within the microtissues. They concluded that the SF-CMTs displayed enhanced properties with potential for recellularization and repairment of the heart. Similarly, Ong *et al.* created scaffold-free cardiac patches using multicellular (hiPSC-CMS, CFs, and ECs) cardiac spheroids as building blocks through 3D bioprinting technique.[145] Primitive vessels ($CD31^+$ structures) were found, and implantation onto rat hearts suggested engraftment and vascularization (erythrocytes found in the explanted patch). Overall, these studies demonstrated that the introduction of ECs and CFs in SF-CMTs favors the formation of vascular structures and facilitates the fabrication of cellular constructs with increased sizes.

Other alternatives for enhanced size and tissue vascularization are based on the creation of SF-CMTs with geometries that favor cellular distribution over two dimensions and limit it over the third dimension, resulting in sheet-like constructs.[146] Since the thickness of these constructs does not exceed the diffusion limit ($\sim$200 μm), the cells remain viable. For instance, Okano's group demonstrated that sheet-like SF-CMTs, formed with CMs

Published on 21 July 2020. Downloaded by ASU Library on 2/2/2021 12:58:01 AM.

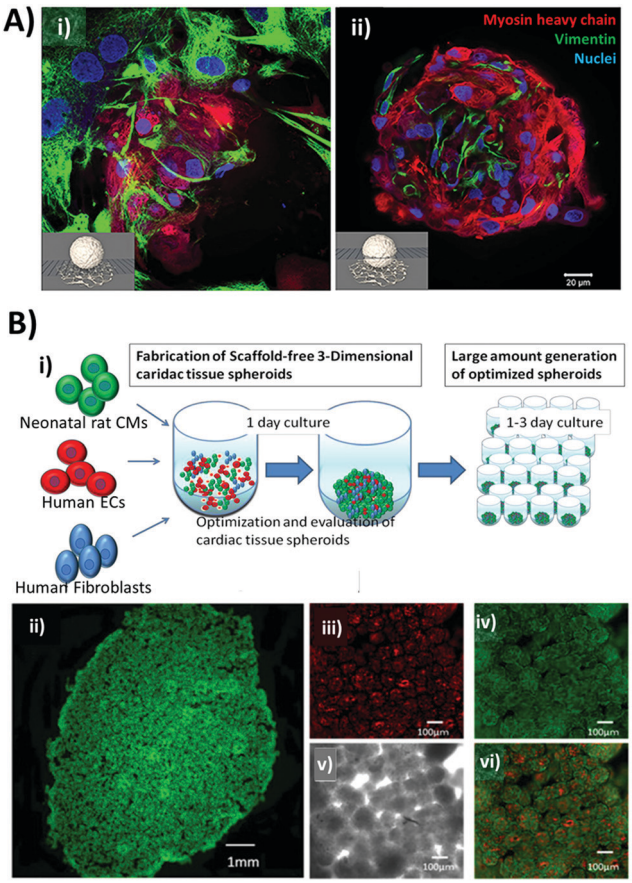

Fig. 3 3D coculture enhances the features of SF-CMTs. (A) Confocal imaging of multicellular cardiac spheroid showing (i) an optical section of the substrate level and (ii) an optical section above the substrate level. (Myosin heavy chain: red, vimentin: green, and nuclei: blue (scale bar = 20 μm)). Adapted with permission from Frontiers [*Front. Mol. Biosci.*], (Beauchamp *et al.*) Copyright © (2020), from ref. 144. (B) Formation of a vascularized cardiac patch, composed of multicellular cardiac spheroids, showing (i) schematic for the fabrication of cardiac spheroids, (ii) contractile cardiac graft fabricated using the prevascularized spheroids, rat neonatal CMs showed in green, (iii) ECs within the cardiac graft (red), (iv) amplification of the rat neonatal CMs (green), (v) phase contrast amplification and (vi) merged image. Adapted with permission from Elsevier [*J. Heart Lung Transpl.*], (Noguchi *et al.*) Copyright © (2016), from ref. 140.

and ECs (ratio 9 : 1), expressed angiogenesis-related genes (vascular endothelial growth factor (VEGF), cyclooxygenase, tyrosine kinase, angiopoietin-1 (Ang-1) and angiopoietin-2 (Ang-2)).[147] Histological analysis further revealed neovascular networks that were maintained and engrafted with the native myocardial tissue upon implantation. The contribution of the cell sheets to neovascularization of the native mouse heart was observed after implantation. Thus, the inclusion of non-CMs in the fabrication of SF-CMTs has proven beneficial as they can help induce neovascularization, paracrine crosstalk with CMs, as well as help to overcome size limitations and engraftment issues.

4.2. Cell composition and fabrication methods of SF-CMTs

There have been mainly two approaches to the fabrication of SF-CMTs. The first is based on guided self-aggregation of terminally differentiated cells, and the second requires the formation of stem cell aggregates and further differentiation into cardiac cells. In either case, the formation of self-assembled cellular aggregates is believed to be driven by thermodynamic processes. In particular, cell culture conditions for the production of SF-CMTs are required to achieve a balance such that the interfacial tensions and adhesion forces between the cells are smaller than those of the cells with the substrate; therefore, the cells are forced to attach between them and arrange in a manner that minimizes the free energy of the system.[148] The availability of adhesion proteins (connexins and cadherins) on the cell surface also plays an important role in minimizing the free energy of the system.[84,149] In 1971, Halbert *et al.* reported, for the first time, that primary CMs have the potential to form self-assembled cell aggregates when cultured on non-adhesive polystyrene surfaces.[150] Since then, several methods have been proposed based on those principles.

One of the early methods utilized for scaffold-free cell culture was the hanging drop technique. The basic principle behind this method consists of placing a cell suspension in a cover glass and inverting it.[150] By doing so, the superficial tension allows for the liquid of the cell suspension to hang from the cover glass. At the same time, gravity forces the cells to gather at the bottom of the droplet, promoting cell-to-cell adhesions and deposition of ECM proteins. For the specific case of cardiac tissue engineering, SF-CMTs can be formed using CMs alone or cocultures of CMs with other cell types.[151] To date, more sophisticated mechanisms have been developed to allow high-throughput and prolonged culture periods.[152,153] Sectioning of these SF-CMTs and further staining enables the identification of cell types and their distribution within the CMTs. Usually, a homogeneous cellular distribution can be found when using terminally differentiated cells. In addition, the deposition of ECM proteins can be confirmed in these spheroids. For example, Beauchamp *et al.* created cardiac spheroids from hiPSC-CMs with varying sizes (2500, 5000, and 10 000 cells per spheroid) using the hanging drop cell culture approach.[154] After three weeks in culture, sectioning, and immunostaining for cardiac-relevant proteins (Connexin 43 (Cx43), myomesin), and a Ca^{2+} handling assay were performed to evaluate the viability and electrophysiological function of the formed SF-CMTs. A homogeneous cell distribution with partially aligned myofibrils was demonstrated, with the cells presenting rounded morphology, reminiscent of those found in the fetal heart. Despite the rounded morphology, the developed SF-CMTs were responsive to pharmacological and electrical stimulations, measured through Ca^{2+} transients. Therefore, they confirmed that it is possible to form cell aggregates from hiPSC-CMs, using the hanging drop method, that respond to exogenous stimuli, rendering this technique a promising approach for the fabrication of SF-CMTs. However, the use of this method presents some disadvantages, for example, changing the culture media and collecting the SF-CMTs can be troublesome due to the small volume of the samples,[155] as well as the obstacle of enhancing CM maturation state.

 This journal is © The Royal Society of Chemistry 2020

Published on 21 July 2020. Downloaded by ASU Library on 2/2/2021 12:58:01 AM.

Microengineered platforms have widely been utilized or designed as a more modern and innovative approach for the development of SF-CMTs in order to overcome some of the challenges of more long-stablished methods such as hanging drop technique.[156] Microfabrication techniques would specifically enable controlled cellular aggregation, uniform size, and geometry of SF-CMTs and continuous media change. Such fabrication methods have permitted the creation of microscale features, such as microwells, with high fidelity and reproducibility to generate SF-CMTs in a high throughput manner.[156] For example, Cha *et al.* utilized photolithography and soft lithography methods to create cylindrical microwells with inverted-pyramidal openings.[157] They created a silicon (Si) master mold through a series of etching steps. Then, polydimethylsiloxane (PDMS) was used to create a negative replica of the Si master mold, which was in turn used as a stamp over polyethylene glycol (PEG) hydrogel to cast the final microwell array. Human MSCs were seeded at a density of 2×10^5 to 6×10^5 cells per array to test the feasibility of the platform. Uniform-sized spheroids with diameters ranging from 100 to 180 μm were created, depending on the cellular seeding density. This platform offered a simple method for the creation of spheroids with highly controlled cell number and size. Other similar approaches based on soft-lithography were also implemented by casting agarose hydrogel using elastomeric stamps or molds.[158,159] The low cellular adhesion to the agarose surface enables self-cellular aggregation, inducing cell-to-cell adhesions for the formation of cellular constructs. Additionally, the high fidelity of agarose casting (down to micrometer scale) allows for the precise creation of microwells of varying shapes and sizes.

Agarose and other hydrogels (*i.e.* methylcellulose hydrogel) have been alternatively used for coating cell culture plates, producing ultra-low adhesion surfaces for inducing cell aggregation. It is also feasible to induce self-aggregation and form SF-CMTs using polystyrene culture dishes. For instance, Giacomelli *et al.* seeded hiPSC-CMs and hiPSC-derived ECs ($CD34^+$) on conical 96-well plates in order to fabricate complex multicellular SF-CMTs.[160] They used different ratios of hiPSC-CMs:ECs to evaluate the optimal composition. It was found that the composition that led to the best organization and distribution of the $CD34^+$ cells was 85% : 15% (of hiPSC-CMs : ECs, respectively) (Fig. 4A(i and ii)). Further qRT-PCR analysis of hiPSC-CMs:ECs SF-CMTs showed significant changes in expression of genes relevant for the cardiac function, specifically, the upregulation of sarcomeric structural genes, ion-channel genes, and Ca^{2+} handling genes, as compared to the 2D culture of hiPSC-CMs. In a more recent study by the same group, isogenic hiPSC-derived CMs, CFs and ECs were used to form tri-cellular SF-CMTs.[161] It was demonstrated that the inclusion of hiPSC-CFs improved the maturation of the hiPSC-CMs (enhanced cellular structures, mitochondrial metabolism, and electrophysiological features), through the cellular coupling mediated by gap junctions between the hiPSC-CMs and hiPSC-CFs and tri-cellular crosstalk. These results confirmed that the coculture of cells can enhance features relevant for SF-CMTs. In a similar fashion, Ravenscroft *et al.* formed spheroids composed of a combination of hESC-CMs or hiPSC-CMs, and non-myocyte (dermal ECs, coronary artery ECs, and CFs) using round bottom ultra-low adhesion plates (Fig. 4B(i–vi)).[162] They assessed the contribution of non-myocytes to the state of maturation of both hESC-CMs and hiPSC-CMs cultured in SF-CMTs. Cardiac-marker immunostaining of SF-CMTs revealed enhanced striations in the CMs cocultured with ECs and CFs (Fig. 4B(iv)). Significantly increased expression of S100A1 and TCAP (markers for sarcomere assembly), PDE3A and KCND3 (markers for cardiovascular function), and NOS3 (nitric oxide production) were found in multicellular SF-CMTs, suggesting crosstalk between non-myocytes and hiPSC-CMs. Also, higher amplitude Ca^{2+} transients and improved

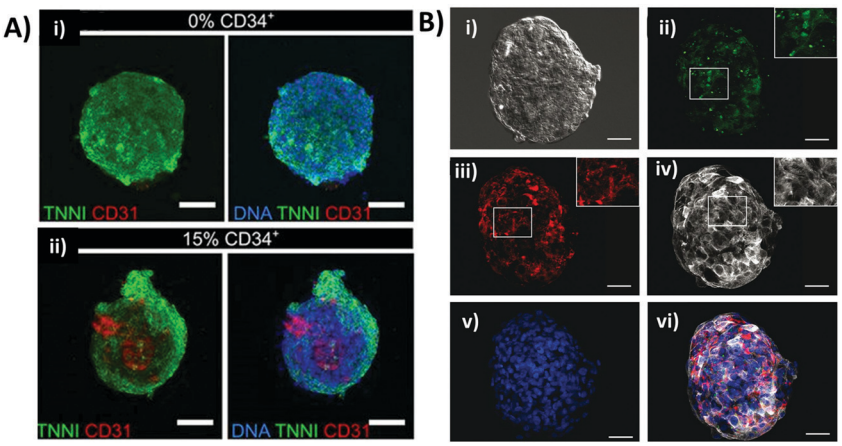

Fig. 4 Fabrication of SF-CMT using low-adhesion surfaces. (A) SF-CMT formed using hiPSC-CMs (i) only (green) and (ii) SF-CMT formed using a ratio of 85% of hiPSC-CMs and 15% of $CD34^+$ cells (green and red respectively). (Scale bars: 100 μm.) Adapted with permission from The Company Of Biologists Ltd. [Development], (Giacomelli *et al.*) Copyright © (2017), from ref. 160. (B) Multicellular SF-CMT fabricated using low-adhesion surfaces (i) DIC image of a multicellular SF-CMT formed with (ii) ECs (CD31: green), (iii) fibroblasts (collagen I: red) and (iv) CMs (ACTN2: white), (v) the nuclei of the cells (blue), and (vi) merged image. (Scale bars: 50 μm.) Adapted with permission from Oxford University Press [*Toxicol. Sci.*], (Ravenscroft *et al.*) Copyright © (2016), from ref. 162.

Published on 21 July 2020. Downloaded by ASU Library on 2/2/2021 12:58:01 AM.

caffeine response was found in multicellular SF-CMTs when compared to SF-CMTs composed of monoculture of CMs. However, CMs in the multicellular SF-CMTs still lacked structural maturity.

A different approach for the fabrication of SF-CMTs involves the use of a temperature-responsive polymer, namely poly(*N*-isopropyl acrylamide) (PIPAAm).[163] In a relevant work by Okano's group, PIPAAm was used for coating polystyrene culture dishes to create a surface that was slightly hydrophobic and promoted cell adhesion at 37 °C but reversed to hydrophilic and non-adhesive at 20 °C[164] (Fig. 5A(i)). When MSCs were seeded on these surfaces, they formed cell-to-cell adhesions and coupling, resulting in the formation of scaffold-free microtissues. In a similar work, Sakaguchi *et al.*[141] demonstrated that multicellular sheets could be stacked, up to 12-layers, to form thicker microtissues. When layered, the cell sheets formed networks of vascular capillaries interspersed between layers. In another study, Chang *et al.* created multilayered cell sheets formed with MSCs and transplanted them on the surface of the LV of porcine models.[165] It was demonstrated that the implanted cell sheets successfully adhered to the host cardiac tissue (Fig. 5(ii–v)). Furthermore, Masumoto *et al.* demonstrated the possibility to form cardiac cell sheets with unpurified hiPSC-CMs.[166] The engineered hiPSC-CM cell sheets were transplanted to a rat model of sub-acute MI to test their regenerative capacity, leading to improved systolic function and LV FS after transplantation. Notably, the implants were able to engraft with the host myocardium, with an accumulation of vWF^+ ECs around the graft, suggesting neovascularization mediated by the transplanted cells (Fig. 5B(i and ii)). These approaches confirmed the efficacy of cell sheets as an efficient strategy for the fabrication of SF-CMTs with multicellular constructs and controlled size for cardiac regeneration. However, no direct evidence of electrical coupling has been found between the SF-CMTs and the host myocardium upon implantation.

SF-CMTs can also be derived from the directed differentiation of embryoid bodies (EBs). EBs, usually in spherical geometry, are cellular aggregates formed from pluripotent/multipotent stem cells. EBs were first created for the study of organogenesis and developmental biology, but later their use was expanded for

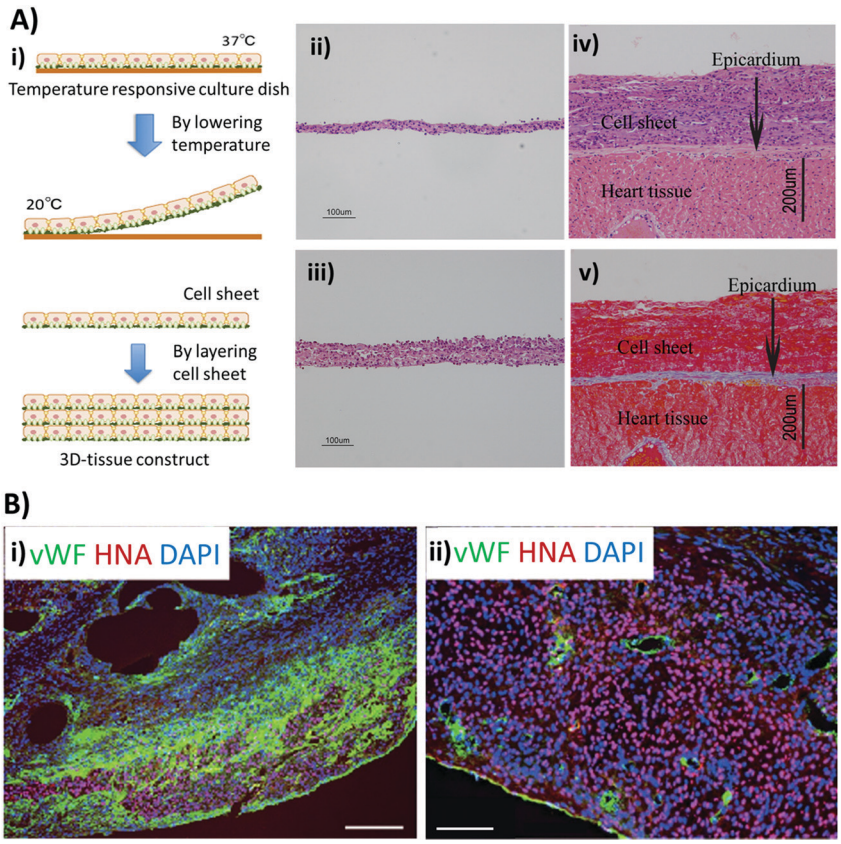

Fig. 5 Fabrication and implantation of SF-CMTs in the form of cell sheets. (A) SF-CMT formed layer by layer using the cell sheet technique (i) diagram for the formation of cardiac cell sheets using temperature-responsive polymeric surfaces. Adapted with permission from Elsevier [*Adv. Drug Delivery Rev.*], (Masuda *et al.*) copyright (2015) [from ref. 164]. (ii) H&E staining of a cross-section of a monolayer MSC cell sheet and (iii) three-layered MSC cell sheet. (iv) H&E staining and (v) Azan staining (collagen-rich areas showed in blue) for three-layered MSC cell sheet 60 minutes after implantation on porcine heart, showing adhesion to the epicardium. Adapted with permission from PLoS ONE [*PLoS ONE*], (Chang *et al.*) Copyright © (2015), from ref. 165. (B) Engraftment of hiPSC-CM sheets in mouse MI model at (i) 3 days, and (ii) 28 days after implantation (green: vWF, red: human cell nuclei (HNA), blue: all nuclei (DAPI)) (scale bars: (i) 200 μm, (ii) 100 μm). Adapted with permission from Springer Nature [*Sci. Rep.*], (Masumoto *et al.*) Copyright © (2014), from ref. 166.

 This journal is © The Royal Society of Chemistry 2020

Published on 21 July 2020. Downloaded by ASU Library on 2/2/2021 12:58:01 AM.

disease modeling, drug screening, and regenerative medicine.[167,168] Conventionally, SF-CMTs derived from EBs are referred to as cardiac organoids as they are composed of multiple types of self-organized cardiac cells that resemble the cell-to-cell interactions of the native myocardium. Adaptations from 2D cardiac differentiation protocols have been implemented to form cardiac organoids from EBs. For example, Yan *et al.* optimized the traditional GiWi protocol[169] (modulation of Wnt/β-catenin canonical signaling pathway) for CM differentiation and applied it to EBs formed with hiPSCs in ultra-low adhesion plates.[170] Spontaneous beating of the organoids was observed upon day ten after initial differentiation, with enhanced expression of sarcomeric α-actinin (SAC) and mature sarcomeric structures when compared with 2D hiPSC-CMs. Cells expressing endothelial markers (CD31 and VE-cadherin) were also found within the organoids, demonstrating the co-differentiation of CMs and ECs in the 3D environment, showing their potential for regenerative medicine due to neovascularization. Different sizes of EBs led to different cell compositions under the same culture and differentiation conditions. This suggests that complex cell-to-cell interactions can influence the Wnt signaling pathway and therefore affect the outcome of 3D differentiation.

The self-organization that occurs within the EB-derived cardiac organoids has been widely studied to gain a better understanding of how these SF-CMTs can be used for biomedical applications. For instance, it was documented by Ma *et al.* that the introduction of biophysical (substrate surface patterned and cell confinement) and biochemical (small molecules for directed differentiation) cues in hiPSC-EBs led to spatial cardiac differentiation.[171] It was observed that the cells in the center of the SF-CMTs expressed cardiac-specific markers (cTnT, SAC, and myosin heavy chain), and the cells in the perimeter expressed myofibroblast markers (SM22, calponin, and smooth muscle actin) (Fig. 6A(i and ii)). The self-organization characteristics prove useful for the development of pre-vascularized SF-CMTs, which in turn may enhance performance for MI treatment.[168] In a different study, Oltolina *et al.* created EBs using human CPCs (hCPCs) obtained from patient samples, using methylcellulose-coated culture wells to induce cell clustering and self-aggregation.[172] Immunostaining of the cell aggregates showed the expression of CPC-related proteins (F-actin, vimentin, CD44, C90, c-Kit, and Sca-1) and ECM proteins (collagen, laminin, and fibronectin) (Fig. 6B(i)). Additionally, expression of cardiac proteins (Cx43, GATA-4 and MEF2C) (Fig. 6B(ii)) and proteins involved in cardiomyogenic programs (YAP and HGF) were found within the SF-CMTs. *In vivo* experiments showed that the SF-CMTs were engrafted after implantation in mice models of MI, and that the hCPCs were able to migrate to the host myocardium and were detectable 7 days after implantation (Fig. 6B(iii)).

The use of dynamic cultures has also been applied for the formation of EBs and differentiation towards cardiac-specific lineage.[173,174] For example, Niebruegge *et al.* created an integrative bioprocess using soft-lithography stamping and a bioreactor system with controlled oxygen concentration for promoting controlled cell expansion, and aggregation and

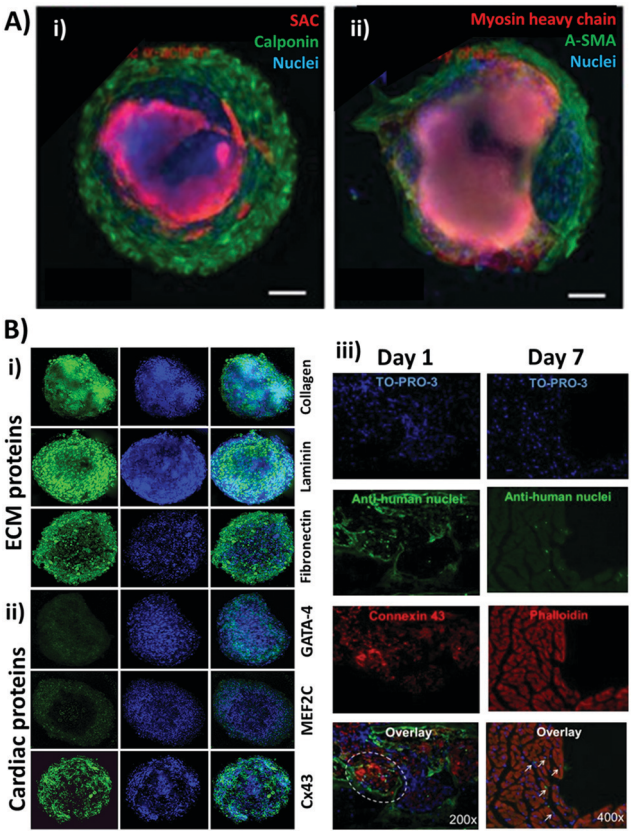

Fig. 6 Spatial cellular organization within EB-derived SF-CMTs. (A) SF-CMT fabrication from the differentiation of EBs, showing CMs in the center and myofibroblasts in the perimeter. (i) SAC: red, calponin: green and DAPI: blue. (ii) Myosin heavy chain: red, smooth muscle actin: green, DAPI: blue. (Scale bars: 100 μm). Adapted with permission from Springer Nature [*Nat. Commun.*], (Ma *et al.*) Copyright © (2015), from ref. 171. (B) immunostaining of hCPC-derived SF-CMTs, showing expression of (i) ECM proteins, and (ii) cardiac proteins (scale bar: 50 μm). (iii) Sections of injured mice myocardium implanted with hCPC-derived SF-CMTs (showed in green) at 1 day (left panel) and 7 days (right panel) after implantation. Circle showing engrafted spheroids and arrows showing dispersed hCPCs. Adapted with permission from PLoS ONE [*PLoS ONE*], (Oltolina *et al.*) Copyright © (2015), from ref. 172.

differentiation of hESCs.[175] The differentiation was performed through suspending the cells in differentiation medium within the bioreactor. Upregulation of cardiac-specific genes, specifically SAC, cTnT, and MLC2v, was found in the microtissues formed 14 days after the start of differentiation. It was suggested that this system could be translated for cardiac differentiation of hiPSCs as well. Hence, the formation of EBs and further 3D cardiac differentiation proves to be another viable method in the obtention of multicellular SF-CMTs with tissue-level relevant characteristics including function and structure.

5. Nanoengineering approaches in cardiac tissue engineering

The unique characteristics of nanoscaled materials (*i.e.*, nanomaterials) and their integration with tissue engineering approaches

Published on 21 July 2020. Downloaded by ASU Library on 2/2/2021 12:58:01 AM.

has proved their potential to enhance the functionalities of engineered CMTs.[176] Through improving the microenvironment of the SF-CMTs, in particular using nanomaterials, it is possible to better mimic the characteristics of the native myocardium, toward a more mature phenotype of *in vitro* and better functionalities *in vivo*. The addition of nanomaterials to stem cell culture, specifically, can modulate their differentiation and fate.[177] Carbon-based and gold-based nanomaterials have been amongst the most popular nanomaterials for cardiac tissue engineering due to their conductive electrical properties.[102–104,178–183] Other nanomaterials have also been used for the construction of CMTs, for example, silicon nanoparticles, polymeric nanofibers, and iron-based magnetic nanoparticles.[184] Whereas a myriad of nanomaterials exists, not all may be suitable for interactions with cardiac cells, as these nanomaterials need to meet specific criteria such as biocompatibility, lack of immunogenicity and cytotoxicity, *etc.* For example, it has been reported that carbon-based nanomaterials such as carbon nanotubes (CNTs) are more prone to elicit immune reactions (inflammation and formation of granulation tissue) and toxicity[178] as opposed to gold-based nanomaterials, which show better biocompatibility.[176,185–188] In addition, key advantages of gold nanomaterials include a diverse nanoscale architecture, in the form of nanoparticles, nanorods, or nanowires, facile fabrication processes, as well as excellent surface properties amenable for assembly of functional groups.[189,190] The extent of the immune reaction and cytotoxicity to some nanomaterials has also been linked to their size, geometry, surface chemistry, concentration and the rate at which they are cleared by the immune system.[191] The main cytotoxic mechanism is due to the cellular uptake of the nanoparticles and their capacity to induce cellular oxidative stress, causing damage to the DNA and cytoplasmic components, and triggering apoptosis.[192] In order to increase the biocompatibility of nanomaterials, several alterations have been proposed, such as surface modifications and functionalization with biocompatible polymers, since polymers play an important role in protein adsorption,[193] cell membrane interactions, and cellular uptake. For example, polyethylene glycol (PEG), poly(ethylene glycol)-*co*-poly(D,L-lactide) (PELA),[194] and poly(acrylic acid)[195] are among some of the polymers used for surface functionalization of nanomaterials. In the following section, we discuss reports of diverse approaches for the utilization of nanomaterials towards the engineering of SF-CMTs.

5.1. Integration of scaffold-free cardiac microtissues (SF-CMTs) with nanomaterials

To date, several approaches have proposed the use of nanomaterials in conjunction with SF-CMTs to enhance their function and maturation. For instance, Tan *et al.* utilized agarose microwells to create SF-CMTs composed of neonatal rat CMs or hiPSC-CMs and added electrically conductive Si nanowires (SiNWs) (diameter ≈ 100 nm; length ≈ 10 μm) at a ratio of 1 : 1 to the cells (CMs : SiNWs)[196] (Fig. 7A). TEM imaging revealed that the SiNWs localized in the intercellular space within SF-CMTs, which has been suggested to improve cell-to-cell coupling. The influence of the synergistic effect of 3D culture and the addition of SiNWs to CMs maturation was then evaluated. It was found that the presence of SiNWs promoted the expression of SAC, cTnI, Cx43, and beta myosin heavy chain

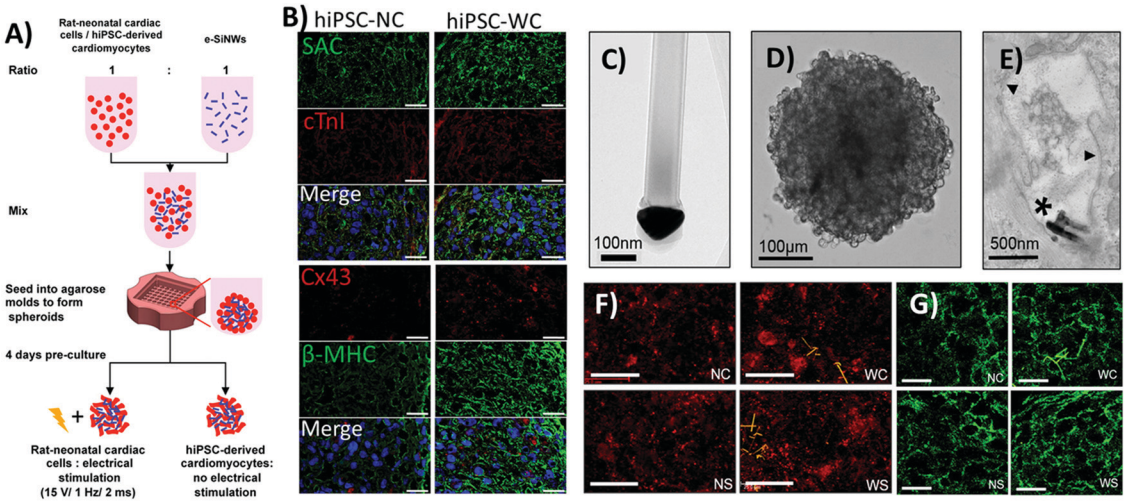

Fig. 7 Fabrication of rat and hiPSC-CM spheroids with SiNWs. (A) Diagram for the fabrication of the SF-CMTs with SiNWs. (B) Immunostaining for SAC and cTnI, Cx43 and β-MHC in hiPSC-CMs spheroids with and without SiNWs (scale bars: 20 μm). Experimental groups: hiPSC-CMs spheroids without SiNWs and no stimulation (hiPSC-NC); hiPSC-CMs spheroids with SiNWs and no stimulation (hiPSC-WC). Adapted with permission from the American Chemical Society [*Nano Lett.*], (Tan *et al.*) Copyright © (2015), from ref. 196. (C) TEM image of the SiNWs. (D) hiPSC SF-CMTs with SiNWs on day 0 after fabrication. (E) TEM image of a spheroid section and SiNWs localization in the extracellular space. Asterisk, nanowire location; triangle, cell membrane. (F) Immunostaining for Cx43 (red) expression (SiNWs shown in yellow). (G) Immunostaining for N-cad (green) expression. Experimental groups: spheroids without SiNWs and unstimulated at day 19 (NC); spheroids with SiNWs and unstimulated at day 19 (WC); Spheroids without SiNWs and stimulated at day 19 (NS); Spheroids with SiNWs and stimulated at day 19 (WS). Adapted with permission from the American Chemical Society [*Nano Lett.*], (Richards *et al.*) Copyright © (2016), from ref. 197.

 This journal is © The Royal Society of Chemistry 2020

Published on 21 July 2020. Downloaded by ASU Library on 2/2/2021 12:58:01 AM.

(β-MHC) (Fig. 7B), and the upregulation of Ca^{2+} channel coding genes (CACNA1C/CACNA1G), which led to improved Ca^{2+} handling. Additionally, enhanced sarcomere ultrastructure (increased Z-line width and alignment, and increased SAC length) were observed in SF-CMTs fabricated with hiPSC-CMs. Furthermore, the authors investigated the effect of electrical stimulation on the neonatal rat SF-CMTs, with a stimulation regime of 15 V at 1 Hz, 2 ms pulses to mimic electrical signals within the heart. SF-CMTs with SiNWs were found to have significantly improved amplitude contraction and synchronization (measured through fractional area change) upon exposure to electrical stimulation. Also, a significantly higher expression of Cx43 was present in SF-CMTs incorporated with SiNWs, which potentially explained the improved electrical propagation within the cellular construct. It was hypothesized that the SiNWs propitiated the formation of an anisotropic mechanical microenvironment, thereby inducing an enhanced alignment of the intracellular contractile apparatus, and therefore improved electrical features of the SF-CMTs. In another study by the same group, they investigated the effect of electrical stimulation in SF-CMTs composed of hiPSC-CMs and SiNWs[197] (Fig. 7C–E). An electrical stimulation regime (2.5 V cm^{-1}, 1 Hz, 5 ms pulses) was used to mimic the electrical signals generated by the sinoatrial node in the heart. The hiPSC-CMs that were incorporated with SiNWs and exposed to electrical stimulation displayed significantly higher expression of Cx43 (Fig. 7F) and N-cadherin (N-cad) (Fig. 7G) when compared to the control groups, suggesting the formation of functional cell-to-cell junctions that allow for improved electrical signal propagation and mechanical coupling. Cardiac-specific marker immunostaining further revealed that the addition of SiNWs improved sarcomere quality (denoted by SAC striation) and induced an increase in the ratio of β-MHC to alpha myosin heavy chain (α-MHC), demonstrating a more mature phenotype. Significantly higher levels of ventricular myosin light chain protein were observed in the electrically stimulated groups, suggesting that the electrical stimulation induced a ventricular-like phenotype in hiPSC-CMs, as further corroborated with an observed reduction in the spontaneous beating rate. In general, the authors demonstrated that the effects of electrical stimulation on hiPSC-CMs can be enhanced by the presence of an electrically conductive microenvironment induced by SiNWs, where the combination of electrically conductive nanoparticles and electrical stimulation in SF-CMTs led to a more mature ventricle-like phenotype in hiPSC-CMs.

In a study by Park *et al.*, scaffold-free tissue spheroids were formed from MSCs using the hanging drop technique, and further enriched with reduced graphene oxide flakes (RGO)[198] (Fig. 8B(i and ii)). The addition of RGO increased the expression of VEGF and Cx43 within the spheroids. An enhanced vascularization of the infarcted myocardium was found after the implantation of the hybrid MSC-RGO spheroids in mice MI model, presumably due to the secretion of growth factors (*i.e.*, vWF) (Fig. 8B(iii)). Additionally, LVEF was improved, and fibrosis was decreased in the infarct zone (Fig. 8B(iv)). Increased expression of Cx43 was also found in the infarct border zone (Fig. 8B(v)).

In a study by Ahadian *et al.*, EBs were created from 129/SEV-derived mouse stem cells using hanging drop technique, and the influence of the addition of graphene on directed cardiac differentiation was investigated[199] (Fig. 8A). During cell seeding, the EBs were enriched with graphene, at a concentration of either 0.1 mg mL^{-1} or 0.2 mg mL^{-1}. Phase-contrast imaging after three days of culture showed the presence of fragments of graphene sheets distributed throughout the EBs. Lower impedance was found in the EBs enriched with 0.2 mg mL^{-1} (298 kΩ) or 0.1 mg mL^{-1} (665 kΩ) of graphene when compared to the control group (0 mg mL^{-1} graphene) (928 kΩ). Stiffness of the EBs was further measured using atomic force microscopy (AFM), revealing that the addition of graphene increased the Young's modulus of the microtissues (31 ± 1.7 kPa, compared to control = 26.8 ± 4.4 kPa). Four days after seeding, the 0.2 mg mL^{-1} graphene-incorporated EBs were subjected to an electrical stimulation regime (4 V, 1 Hz, 10 ms). Significantly higher expression of cTnT was found in electrically stimulated EBs, while within this group, the graphene-incorporated EBs exhibited significantly enhanced expression of cTnT as compared to the control condition (EBs with no graphene) (Fig. 8C). Significant upregulation of cardiac-specific genes (cCTC1, MYH6, MYH7, and TNNT2) and spontaneous beating was also found in graphene-incorporated EBs. Additionally, more organized sarcomeric structures were observed in the cells within the stimulated EBs incorporated with graphene as compared to pristine EBs. The outcome of this study demonstrated that inducing an electromechanical microenvironment, relevant to the myocardium, by the combination of graphene sheets and electrical stimulation can lead to cardiac differentiation without the need of addition of soluble factors or small molecules.

Overall, the integration of nanomaterials and SF-CMTs has shown enhanced cell-to-cell interactions,[196,197] and cell-to-ECM interactions.[198] Specifically, the integration of electrical stimulation to the SF-CMTs enriched with nanomaterials has proved beneficial to improve their electrophysiological properties and increase the expression of cardiac-specific proteins. It has been suggested that the introduction of physiologically relevant electrical cues in combination with electrically conductive nanomaterials creates a microenvironment within the SF-CMTs that facilitates electrical propagation and closely mimics the microenvironment of the heart.[199] Improving the different cellular interactions and the microenvironment within the SF-CMTs is paramount to overcome the current challenges of cell-based therapies as well as engineering of mature and functional SF-CMTs for cardiac therapy. Before these approaches proceed to clinical trials, more fundamental investigations are needed to elucidate the action mechanism of specific nanoparticles and the influence of other possible biochemical or biophysical signaling cues in a more complex tissue environment (*i.e.*, at an organ level). Moreover, it is necessary to reach a consensus on the optimal concentration of nanoparticles to be added to SF-CMTs since it has been demonstrated that the outcome is highly dose-dependent. So far, the concentrations used vary widely from study to study, and while the main objective is to avoid cytotoxicity, there is still room for optimization. In addition, the long-term

Published on 21 July 2020. Downloaded by ASU Library on 2/2/2021 12:58:01 AM.

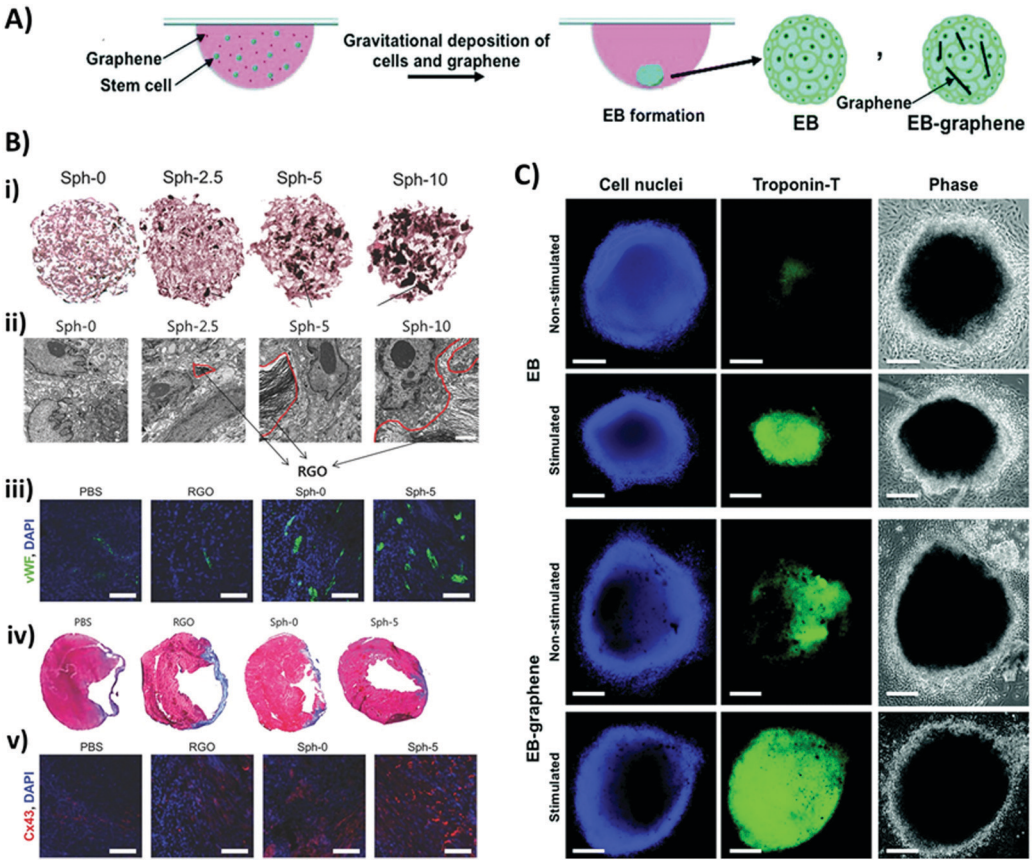

Fig. 8 Integration of graphene sheets and RGO flakes into EBs. (A) Diagram of EB formation through hanging-drop technique. Adapted with permission from the Royal Society of Chemistry [*Nanoscale*], (Ahadian *et al.*) Copyright © (2016), from ref. 199. (B) formation and implantation of hybrid SF-CMTs with RGO flakes (i) H&E stain of spheroids formed with different concentrations of RGO (shown in black) (scale bar: 100 μm). (ii) TEM images of spheroids formed with different concentrations of RGO (arrows). (Scale bar: 2 μm.) (iii) Assessment of capillary density by immunostaining of VWF (scale bars: 100 μm). (iv) Masson's trichrome staining of explanted hearts indicating fibrotic areas (blue). (v) Expression of Cx43 in the infarct border zone (scale bars: 100 μm). Experimental groups: injection of PBS (PBS), injection of RGO flakes (RGO), injection of MSC spheroids (Sph-0), and injection of MSC–RGO hybrid spheroids (Sph-5). Adapted with permission from Wiley-VCH Verlag GmbH & Co [*Adv. Funct. Mater.*], (Park *et al.*) Copyright © (2015), from ref. 198. (C) Expression of cTnT (green) in EB-derived SF-CMTs. (Scale bars: 100 μm.) Experimental groups: EBs formed without the addition of graphene without and with electrical stimulation respectively: EB (non-stimulated and stimulated). EBs formed adding graphene without and with electrical stimulation respectively: EB-graphene (non-stimulated and stimulated). Adapted with permission from the Royal Society of Chemistry [*Nanoscale*], (Ahadian *et al.*) Copyright © (2016), from ref. 199.

effects towards the host myocardium need to be investigated. So far, bioaccumulation of nanomaterials in the cardiac tissue and the possible side effects due to the implantation of SF-CMTs enriched with nanomaterials have not yet been reported, since those studies were performed *in vitro*. Thus, a balance between having the maximal beneficial effect and avoiding cytotoxic concentrations needs to be reached.

6. Summary and future directions

In this review article, we summarized different regenerative-medicine approaches developed towards cardiac repair therapies. Traditional therapies based on drug treatment are focused mainly on the protection of the remaining viable myocardium and deceleration of fibrotic remodeling. Currently, when drug-based therapies fail, few alternatives remain.[20] Inducing regeneration of the damaged myocardium is not trivial and presents several challenges. Thus, emerging alternative treatments have mainly focused on the recellularization of the damaged cardiac tissue and the promotion of endogenous repair mechanisms (Table 1). The more straightforward methods are based on the delivery of dissociated cells in suspension to the myocardium. The findings of several cell-based cardiac therapies have suggested that the main role of the implanted cells resides in paracrine signaling and crosstalk with the native tissue. Therefore, it has been shown that independent of the source, cell-based therapies moderately promote neovascularization and repress the formation of fibrotic tissue, thus providing cardioprotective effects but not fully recellularizing the myocardium. The main challenges of cell-based therapies are the stress induced on cells from delivery to the myocardium that leads to low cellular survival and retention, poor engraftment, and the risk of delivery to non-target sites/organs.

Tissue engineering approaches have mainly focused on integrating engineering and biology for the development of

 This journal is © The Royal Society of Chemistry 2020

Published on 21 July 2020. Downloaded by ASU Library on 2/2/2021 12:58:01 AM.

Table 1 Summary table of the main characteristics of alternative approaches for cardiac repair

	Cell-based cardiac therapy	Scaffold-based cardiac microtissues (SB-CMTs)	Scaffold-free cardiac microtissues (SF-CMTs)
Size and geometry	Dissociated cells in suspension.	Patches or sheet-like tissues (up to 1–2 cm per side and up to 1–2 mm thickness)	Spheroids (up to 500 μm diameter) or sheet-like tissues (up to 400 μm thickness)
Cellular composition	Single cell type administered at a time.	Mainly CMs (hiPSC- or hESC-derived), occasionally enriched with other types of cells such as endothelial cells, and cardiac fibroblasts.	Mainly CMs (hiPSC- or hESC-derived), enriched with endothelial cells, cardiac fibroblasts and occasionally stem cells.
Delivery method	Intracoronary or intramyocardial injection.	Thoracotomy surgery or thoracoscopy.	Intramyocardial injection or thoracotomy surgery.
Exogenous materials	Not common	Scaffolds from diverse types of biomaterials such as natural or synthetic polymers, hydrogels, electrospun fibers, composite biomaterials often incorporated with nanomaterials.	Occasional inclusion of electrically conductive nanomaterials, such as graphene and graphene oxide flakes, and conductive Si nanowires.
Preparation and fabrication method	*In vitro* cellular purification and expansion, followed by dissociation prior injection.	*In vitro* cellular expansion, differentiation, and purification (when applicable) followed by encapsulation or seeding on the scaffold. Electrical stimulation in some cases.	*In vitro* cellular expansion, differentiation, and purification (when applicable) followed by induced self-aggregation. Or formation of EBs followed by 3D differentiation. Electrical stimulation in some cases.
Trial phase	Several preclinical studies have been performed and some phase I clinical trials.	Several preclinical studies have been performed and few Phase I clinical trials.	Several preclinical studies have been performed.
Reported effects *in vivo*	Paracrine signaling inducing neovascularization in the borders of the infarcted zone.	Potential for remuscularization, paracrine signaling, induction of neovascularization, reduction of infarct size.	Cardioprotection, paracrine signaling, induction of neovascularization, reduced fibrotic remodeling.
Main challenges	Poor cellular survival and retention after implantation. Non-targeted delivery. Poor remuscularization potential. Lack of control of cellular differentiation after implantation.	Invasive delivery. Optimal engineering of scaffold in terms of chemical composition, stiffness, degradation rate and immunogenic activity. Immature state of hiPSC- and hESC-derived cells.	Immature state of hiPSC- and hESC-derived cells. Need of further optimization for size and cellular composition. Need of further investigation regarding the use of nanomaterials.

robust cellular constructs and tissue surrogates in order to overcome the critical challenges of cell-based therapeutic methods. The prominent recent cell types used in this category are stem cell-derived cells (CMs, ECs, CFs), and recently hiPSC-CMs due to the potential use of allograft cells for regeneration. The optimized culture of hiPSC-derived cells has helped to make advancements towards the formation of functional CMTs. At the same time, enhancing the resemblance of the architecture of CMTs to the native myocardium has led to enhanced maturation of hiPSC-derived cells and promoted cell-to-cell interactions within the tissue environment. Biomaterials from diverse origins, natural or synthetic with precisely controlled stiffness, chemical moieties, *etc.*, have been used as scaffolding matrices in the formation of SB-CMTs. However, challenges for the use of SB-CMTs in clinical applications include the introduction of exogenous biomaterials to the host tissue that can elicit immune responses or cytotoxicity, lack of engraftment and cellular coupling, and often the requirement of surgically invasive interventions to implant the engineered tissue constructs.

To address the current limitations of cell-based and scaffold-based tissue engineering strategies, in the past few years, engineering of SF-CMTs has emerged as potentially powerful approach for the treatment of MI with minimally invasive implantation procedures. The use of coculture and fabrication of multicellular constructs/organoids has proved optimal, as such cellular composition could better resemble the native myocardium. Also, paracrine and endocrine signaling is enhanced in SF-CMTs, which lead to a more mature state of hiPSC-derived cells. Several methods for the construction of SF-CMTs have been proposed, based on the promotion of cell aggregation through inducing cell-to-cell adhesion and electromechanical coupling. These methods can be divided into three broad categories, with the first group consisting of gravity-assisted methods, either using conventional hanging drop technique or microengineered platforms, that rely on gravity to form cellular aggregates out of cell suspensions.[150,152] Usually, these methods offer great control on SF-CMT size and cell number, allowing for homogeneous formation of spheroids. The second group involves the use of ultra-low adherent surfaces, such as PIPAAm-coated surfaces, to promote cell aggregation through the balance of electrostatic forces and reduction of free-energy. The fabrication of SF-CMTs using low attachment substrates requires minimal manipulation of the cell aggregates, which translates to lower stress induced by handling. The last group is based on the obtention of SF-CMTs through the differentiation of EBs. The main advantages of this method are the resultant physiologically-relevant cellular composition and organization,[171,200] and the ease of scaling to high-throughput output; however, controlling the size can be problematic.

Despite significant promise, before the extended use of SF-CMTs in clinical trials, several remaining challenges need to be addressed. First, the maturation state of the stem cell-derived CMs needs to be improved. The advancement of *in vitro* maturation techniques may lead to more robust SF-CMTs that better resemble the adult myocardium, and consequently, may

Published on 21 July 2020. Downloaded by ASU Library on 2/2/2021 12:58:01 AM.

lead to better engraftment and retention within the native tissue. In addition, there is a need to elucidate the mechanisms of the delivery of the SF-CMTs since it has been reported that it can have consequences in the engraftment and electrical coupling of the implanted cells. According to some studies, the intramyocardial delivery of spherical SF-CMTs may be the best option for enhanced electrical coupling.[201,202] Still, more studies are necessary in order to standardize the optimal size and delivery method to the infarcted myocardium. Recent approaches have utilized exogenous cues such as nanomaterials to enhance the structural maturity and functionalities of SF-CMTs. However, detailed studies are required to unveil the nanomaterials' specific mechanisms of action on cellular- and tissue-level function within the heart, since it has been reported that some nanomaterials can elicit toxic reactions, such as foreign body reaction, inflammation, and apoptosis among others, in different organs in preclinical studies.[203] The cellular composition within the engineered SF-CMTs needs to be determined in a manner that optimizes the electromechanical properties as well as the paracrine signaling of the tissue. Additionally, non-targeted delivery and teratogenic potential of the implanted cells need to be thoroughly studied and addressed, since it has been reported that hiPSC-derived SF-CMTs can induce immune rejection in some cases and can also lead to the formation of malignant teratocarcinomas *in vivo*.[204] Overall, the development of SF-CMTs holds great potential for myocardial repair therapy and treatment of MI, due to their enhanced structure, tissue organization, and cellular composition, and the lack of exogenous bulk materials. Additionally, the effects of the introduction of nanomaterials to the fabrication of SF-CMTs are worthy of further investigation due to their proven potential for the enhancement of their electrophysiological features. With this, we anticipate that the inclusion of nanomaterials and nanoengineering methods will lead to the next generation of SF-CMTs for cardiac regenerative medicine.

Conflicts of interest

There are no conflicts of interest to declare.

Acknowledgements

The authors would like to acknowledge the Arizona Biomedical Research Commission (ABRC) New Investigator Award # AWD32676, NIH Award # 1R21EB028396-01 and NSF CAREER Award # 1653193.

References

1 S. S. Virani, A. Alonso, E. J. Benjamin, M. S. Bittencourt, C. W. Callaway, A. P. Carson, A. M. Chamberlain, A. R. Chang, S. Cheng and F. N. Delling, *Circulation*, 2020, E139–E596.
2 G. Savarese and L. H. Lund, *Card. Fail. Rev.*, 2017, **3**, 7.
3 E. J. Benjamin, M. J. Blaha, S. E. Chiuve, M. Cushman, S. R. Das, R. Deo, S. D. de Ferranti, J. Floyd, M. Fornage, C. Gillespie, C. R. Isasi, M. C. Jimenez, L. C. Jordan, S. E. Judd, D. Lackland, J. H. Lichtman, L. Lisabeth, S. M. Liu, C. T. Longenecker, R. H. Mackey, K. Matsushita, D. Mozaffarian, M. E. Mussolino, K. Nasir, R. W. Neumar, L. Palaniappan, D. K. Pandey, R. R. Thiagarajan, M. J. Reeves, M. Ritchey, C. J. Rodriguez, G. A. Roth, W. D. Rosamond, C. Sasson, A. Towfighi, C. W. Tsao, M. B. Turner, S. S. Virani, J. H. Voeks, J. Z. Willey, J. T. Wilkins, J. H. Y. Wu, H. M. Alger, S. S. Wong, P. Muntner and American Heart Association Statistics Committee and Stroke Statistics Subcommittee, *Circulation*, 2017, **135**, E146–E603.
4 M. A. Laflamme and C. E. Murry, *Nature*, 2011, **473**, 326–335.
5 E. G. Nabel and E. Braunwald, *N. Engl. J. Med.*, 2012, **366**, 54–63.
6 S. L. Jackson, X. Tong, R. J. King, F. Loustalot, Y. Hong and M. D. Ritchey, *Circ. Heart Fail.*, 2018, **11**, e004873.
7 B. Ziaeian and G. C. Fonarow, *Nat. Rev. Cardiol.*, 2016, **13**, 368–378.
8 A. A. Inamdar and A. C. Inamdar, *J. Clin. Med.*, 2016, **5**, 62.
9 E. De Angelis, M. Pecoraro, M. R. Rusciano, M. Ciccarelli and A. Popolo, *Int. J. Mol. Sci.*, 2019, **20**(7), 1698.
10 E. Braunwald, *JACC Heart Fail.*, 2013, **1**, 1–20.
11 J. I. Virag and C. E. Murry, *Am. J. Pathol.*, 2003, **163**, 2433–2440.
12 S. D. Prabhu and N. G. Frangogiannis, *Circ. Res.*, 2016, **119**, 91–112.
13 K. Thygesen, J. S. Alpert and H. D. White, *Circulation*, 2007, **116**, 2634–2653.
14 H. Z. Zhang, M. H. Kim, J. H. Lim and H.-R. Bae, *J. Korean Med. Sci.*, 2013, **28**, 402–408.
15 O. Bergmann, R. D. Bhardwaj, S. Bernard, S. Zdunek, F. Barnabé-Heider, S. Walsh, J. Zupicich, K. Alkass, B. A. Buchholz, H. Druid, S. Jovinge and J. Frisén, *Science*, 2009, **324**, 98–102.
16 J. P. Cleutjens and E. E. Creemers, *J. Card. Fail.*, 2002, **8**, S344–S348.
17 G. Belostotskaya, M. Hendrikx, M. Galagudza and S. Suchkov, *BioMed Res. Int.*, 2020, **2020**, 7874109, DOI: 10.1155/2020/7874109.
18 H. Maxeiner, N. Krehbiehl, A. Müller, N. Woitasky, H. Akintürk, M. Müller, M. A. Weigand, Y. Abdallah, S. Kasseckert, R. Schreckenberg, K.-D. Schlüter and S. Wenzel, *Eur. J. Heart Failure*, 2010, **12**, 730–737.
19 D. Torella, G. M. Ellison, S. Méndez-Ferrer, B. Ibanez and B. Nadal-Ginard, *Nat. Clin. Pract. Cardiovasc. Med.*, 2006, **3**, S8–S13.
20 A. S. Bhatt, A. P. Ambrosy and E. J. Velazquez, *Curr. Cardiol. Rep.*, 2017, **19**, 71.
21 M. Tonsho, S. Michel, Z. Ahmed, A. Alessandrini and J. C. Madsen, *Cold Spring Harbor Perspect. Med.*, 2014, **4**, a015636.
22 S. Klotz, R. F. Foronjy, M. L. Dickstein, A. Gu, I. M. Garrelds, A. Jan Danser, M. C. Oz, J. D'Armiento and D. Burkhoff, *Circulation*, 2005, **112**, 364–374.

 This journal is © The Royal Society of Chemistry 2020

Published on 21 July 2020. Downloaded by ASU Library on 2/2/2021 12:58:01 AM.

23 X. M. Mueller, *Ann. Thorac. Surg.*, 2004, **77**, 354–362.
24 A. E. S. Shafei, M. A. Ali, H. G. Ghanem, A. I. Shehata, A. A. Abdelgawad, H. R. Handal, K. A. Talaat, A. E. Ashaal and A. S. El-Shal, *J. Gene Med.*, 2017, **19**, e2995.
25 E. C. Perin and J. López, *Nat. Clin. Pract. Cardiovasc. Med.*, 2006, **3**, S110–S113.
26 S. Golpanian, A. Wolf, K. E. Hatzistergos and J. M. Hare, *Physiol. Rev.*, 2016, **96**, 1127–1168.
27 V. F. Segers and R. T. Lee, *Nature*, 2008, **451**, 937–942.
28 A. Behfar, R. Crespo-Diaz, A. Terzic and B. J. Gersh, *Nat. Rev. Cardiol.*, 2014, **11**, 232.
29 A. Ghiroldi, M. Piccoli, F. Cirillo, M. M. Monasky, G. Ciconte, C. Pappone and L. Anastasia, *Int. J. Mol. Sci.*, 2018, **19**, 3194.
30 A. Rodriguez, C. Elabd, E. Amri, G. Ailhaud and C. Dani, *Biochimie*, 2005, **87**, 125–128.
31 R. H. Lee, B. Kim, I. Choi, H. Kim, H. S. Choi, K. Suh, Y. C. Bae and J. S. Jung, *Cell. Physiol. Biochem.*, 2004, **14**, 311–324.
32 S.-L. Chen, W.-W. Fang, F. Ye, Y.-H. Liu, J. Qian, S.-J. Shan, J.-J. Zhang, R. Z. Chunhua, L.-M. Liao and S. Lin, *Am. J. Cardiol.*, 2004, **94**, 92–95.
33 R. R. Makkar, R. R. Smith, K. Cheng, K. Malliaras, L. E. Thomson, D. Berman, L. S. Czer, L. Marbán, A. Mendizabal and P. V. Johnston, *Lancet*, 2012, **379**, 895–904.
34 Q. Sun, Z. Zhang and Z. Sun, *Genes Dis.*, 2014, **1**, 113–119.
35 S. D. Schwartz, J.-P. Hubschman, G. Heilwell, V. Franco-Cardenas, C. K. Pan, R. M. Ostrick, E. Mickunas, R. Gay, I. Klimanskaya and R. Lanza, *Lancet*, 2012, **379**, 713–720.
36 F. Bretzner, F. Gilbert, F. Baylis and R. M. Brownstone, *Cell Stem Cell*, 2011, **8**, 468–475.
37 I. Kehat, D. Kenyagin-Karsenti, M. Snir, H. Segev, M. Amit, A. Gepstein, E. Livne, O. Binah, J. Itskovitz-Eldor and L. Gepstein, *J. Clin. Invest.*, 2001, **108**, 407–414.
38 M. A. Laflamme, K. Y. Chen, A. V. Naumova, V. Muskheli, J. A. Fugate, S. K. Dupras, H. Reinecke, C. Xu, M. Hassanipour and S. Police, *Nat. Biotechnol.*, 2007, **25**, 1015–1024.
39 J. J. Chong, X. Yang, C. W. Don, E. Minami, Y.-W. Liu, J. J. Weyers, W. M. Mahoney, B. Van Biber, S. M. Cook and N. J. Palpant, *Nature*, 2014, **510**, 273–277.
40 Y.-W. Liu, B. Chen, X. Yang, J. A. Fugate, F. A. Kalucki, A. Futakuchi-Tsuchida, L. Couture, K. W. Vogel, C. A. Astley and A. Baldessari, *Nat. Biotechnol.*, 2018, **36**, 597–605.
41 K. Takahashi, K. Tanabe, M. Ohnuki, M. Narita, T. Ichisaka, K. Tomoda and S. Yamanaka, *Cell*, 2007, **131**, 861–872.
42 J. Yu, M. A. Vodyanik, K. Smuga-Otto, J. Antosiewicz-Bourget, J. L. Frane, S. Tian, J. Nie, G. A. Jonsdottir, V. Ruotti and R. Stewart, *Science*, 2007, **318**, 1917–1920.
43 J. Zhang, G. F. Wilson, A. G. Soerens, C. H. Koonce, J. Yu, S. P. Palecek, J. A. Thomson and T. J. Kamp, *Circ. Res.*, 2009, **104**, e30–e41.
44 K. Ban, S. Bae and Y.-S. Yoon, *Theranostics*, 2017, **7**, 2067.
45 S. Mallapaty, *Nature*, 2020, **581**(7808), 249–250.
46 S. Kholia, A. Ranghino, P. Garnieri, T. Lopatina, M. C. Deregibus, P. Rispoli, M. F. Brizzi and G. Camussi, *Vasc. Pharmacol.*, 2016, **86**, 64–70.
47 F. Pagano, V. Picchio, I. Chimenti, A. Sordano, E. De Falco, M. Peruzzi, F. Miraldi, E. Cavarretta, G. B. Zoccai and S. Sciarretta, *Curr. Cardiol. Rep.*, 2019, **21**, 133.
48 A. Kurtz, *Int. J. Stem Cells*, 2008, **1**, 1.
49 M. A. Laflamme and C. E. Murry, *Nat. Biotechnol.*, 2005, **23**, 845–856.
50 X. Wang, W.-c. Xi and F. Wang, *Biotechnol. Lett.*, 2014, **36**, 2163–2168.
51 N. Rezai, S. Y. Corbel, D. Dabiri, A. Kerjner, F. M. Rossi, B. M. McManus and T. J. Podor, *Lab. Invest.*, 2005, **85**, 982–991.
52 C. Robertson, D. D. Tran and S. C. George, *Stem Cells*, 2013, **31**, 829–837.
53 T. Kamakura, T. Makiyama, K. Sasaki, Y. Yoshida, Y. Wuriyanghai, J. Chen, T. Hattori, S. Ohno, T. Kita and M. Horie, *Circ. J.*, 2013, **77**, 1307–1314.
54 V. Volarevic, B. S. Markovic, M. Gazdic, A. Volarevic, N. Jovicic, N. Arsenijevic, L. Armstrong, V. Djonov, M. Lako and M. Stojkovic, *Int. J. Med. Sci.*, 2018, **15**, 36.
55 M. N. Hirt, A. Hansen and T. Eschenhagen, *Circ. Res.*, 2014, **114**, 354–367.
56 J. Veldhuizen, R. Q. Migrino and M. Nikkhah, *J. Biol. Eng.*, 2019, **13**, 29.
57 D. D. Truong, A. Kratz, J. G. Park, E. S. Barrientos, H. Saini, T. Nguyen, B. Pockaj, G. Mouneimne, J. LaBaer and M. Nikkhah, *Cancer Res.*, 2019, **79**, 3139–3151.
58 R. D. Pedde, B. Mirani, A. Navaei, T. Styan, S. Wong, M. Mehrali, A. Thakur, N. K. Mohtaram, A. Bayati and A. Dolatshahi-Pirouz, *Adv. Mater.*, 2017, **29**, 1606061.
59 D. Truong, R. Fiorelli, E. S. Barrientos, E. L. Melendez, N. Sanai, S. Mehta and M. Nikkhah, *Biomaterials*, 2019, **198**, 63–77.
60 K. H. Benam, S. Dauth, B. Hassell, A. Herland, A. Jain, K.-J. Jang, K. Karalis, H. J. Kim, L. MacQueen, R. Mahmoodian, S. Musah, Y.-S. Torisawa, A. D. van der Meer, R. Villenave, M. Yadid, K. K. Parker and D. E. Ingber, *Annu. Rev. Pathol.: Mech. Dis.*, 2015, **10**, 195–262.
61 D. Huh, Y.-s. Torisawa, G. A. Hamilton, H. J. Kim and D. E. Ingber, *Lab Chip*, 2012, **12**, 2156–2164.
62 S. Nagaraju, D. Truong, G. Mouneimne and M. Nikkhah, *Adv. Healthcare Mater.*, 2018, **7**, 1701257.
63 J. Veldhuizen, J. Cutts, D. Brafman, R. Q. Migrino and M. Nikkhah, *Biomaterials*, 2020, 120195.
64 H. K. Voges, R. J. Mills, D. A. Elliott, R. G. Parton, E. R. Porrello and J. E. Hudson, *Development*, 2017, **144**, 1118–1127.
65 C. Zuppinger, *Front. Cardiovasc. Med.*, 2019, **6**, 87, DOI: 10.3389/fcvm.2019.00087.
66 L. Wang, G. Huang, B. Sha, S. Wang, Y. Han, J. Wu, Y. Li, Y. Du, T. Lu and F. Xu, *Curr. Med. Chem.*, 2014, **21**, 2497–2509.
67 J. Huang, Y. Jiang, Y. Ren, Y. Liu, X. Wu, Z. Li and J. Ren, *J. Biomed. Mater. Res., Part A*, 2020, **108**, 1501–1508.

Published on 21 July 2020. Downloaded by ASU Library on 2/2/2021 12:58:01 AM.

68 M. Ravi, V. Paramesh, S. Kaviya, E. Anuradha and F. P. Solomon, *J. Cell. Physiol.*, 2015, **230**, 16–26.
69 N. Annabi, K. Tsang, S. M. Mithieux, M. Nikkhah, A. Ameri, A. Khademhosseini and A. S. Weiss, *Adv. Funct. Mater.*, 2013, **23**, 4950–4959.
70 W. J. Kowalski, F. Yuan, T. Nakane, H. Masumoto, M. Dwenger, F. Ye, J. P. Tinney and B. B. Keller, *Microsc. Microanal.*, 2017, **23**, 826–842.
71 B. Maron, *Br. Heart J.*, 1983, **50**, 1.
72 D. G. Zacharias, T. J. Nelson, P. S. Mueller and C. C. Hook, *Mayo Clin. Proc.*, 2011, **86**, 634–640.
73 Y. Jiang, P. Park, S.-M. Hong and K. Ban, *Mol. Cells*, 2018, **41**, 613.
74 G. J. Scuderi and J. Butcher, *Front. Cell Dev. Biol.*, 2017, **5**, 50.
75 X. Yang, L. Pabon and C. E. Murry, *Circ. Res.*, 2014, **114**, 511–523.
76 W. Keung, K. R. Boheler and R. A. Li, *Stem Cell Res. Ther.*, 2014, **5**, 17.
77 S. D. Lundy, W.-Z. Zhu, M. Regnier and M. A. Laflamme, *Stem Cells Dev.*, 2013, **22**, 1991–2002.
78 T. P. Dias, S. N. Pinto, J. I. Santos, T. G. Fernandes, F. Fernandes, M. M. Diogo, M. Prieto and J. M. Cabral, *Biochem. Biophys. Res. Commun.*, 2018, **499**, 611–617.
79 K. Ronaldson-Bouchard, S. P. Ma, K. Yeager, T. Chen, L. Song, D. Sirabella, K. Morikawa, D. Teles, M. Yazawa and G. Vunjak-Novakovic, *Nature*, 2018, **556**, 239–243.
80 M. C. Ribeiro, L. G. Tertoolen, J. A. Guadix, M. Bellin, G. Kosmidis, C. D'Aniello, J. Monshouwer-Kloots, M.-J. Goumans, Y.-L. Wang and A. W. Feinberg, *Biomaterials*, 2015, **51**, 138–150.
81 D. Zhang, I. Y. Shadrin, J. Lam, H.-Q. Xian, H. R. Snodgrass and N. Bursac, *Biomaterials*, 2013, **34**, 5813–5820.
82 G. D. Lopaschuk and J. S. Jaswal, *J. Cardiovasc. Pharmacol.*, 2010, **56**, 130–140.
83 C. Correia, A. Koshkin, P. Duarte, D. Hu, M. Carido, M. J. Sebastião, P. Gomes-Alves, D. A. Elliott, I. J. Domian and A. P. Teixeira, *Biotechnol. Bioeng.*, 2018, **115**, 630–644.
84 V. J. Bhute, X. Bao, K. K. Dunn, K. R. Knutson, E. C. McCurry, G. Jin, W.-H. Lee, S. Lewis, A. Ikeda and S. P. Palecek, *Theranostics*, 2017, **7**, 2078.
85 S. S. Nunes, J. W. Miklas, J. Liu, R. Aschar-Sobbi, Y. Xiao, B. Zhang, J. Jiang, S. Massé, M. Gagliardi and A. Hsieh, *Nat. Methods*, 2013, **10**, 781.
86 M. Nikkhah, F. Edalat, S. Manoucheri and A. Khademhosseini, *Biomaterials*, 2012, **33**, 5230–5246.
87 P. Zorlutuna, N. Annabi, G. Camci-Unal, M. Nikkhah, J. M. Cha, J. W. Nichol, A. Manbachi, H. Bae, S. Chen and A. Khademhosseini, *Adv. Mater.*, 2012, **24**, 1782–1804.
88 J. Cutts, M. Nikkhah and D. A. Brafman, *Biomarker Insights*, 2015, **10**, S20313.
89 H. Saini, F. S. Sam, M. Kharaziha and M. Nikkhah, *Cell and Material Interface: Advances in Tissue Engineering, Biosensor, Implant, and Imaging Technologies*, 2018, p. 187.
90 A. Pal, B. L. Vernon and M. Nikkhah, *Bioact. Mater.*, 2018, **3**, 389–400.
91 K. Shapira-Schweitzer and D. Seliktar, *Acta Biomater.*, 2007, **3**, 33–41.
92 C. Williams, E. Budina, W. L. Stoppel, K. E. Sullivan, S. Emani, S. M. Emani and L. D. Black III, *Acta Biomater.*, 2015, **14**, 84–95.
93 A. Marsano, R. Maidhof, L. Q. Wan, Y. Wang, J. Gao, N. Tandon and G. Vunjak-Novakovic, *Biotechnol. Prog.*, 2010, **26**, 1382–1390.
94 H. Saini, A. Navaei, A. Van Putten and M. Nikkhah, *Adv. Healthcare Mater.*, 2015, **4**, 1961–1971.
95 Y. W. Chun, D. A. Balikov, T. K. Feaster, C. H. Williams, C. C. Sheng, J.-B. Lee, T. C. Boire, M. D. Neely, L. M. Bellan and K. C. Ess, *Biomaterials*, 2015, **67**, 52–64.
96 P. Sreejit and R. Verma, *Stem Cell Rev. Rep.*, 2013, **9**, 158–171.
97 Y. Miyagi, L. L. Chiu, M. Cimini, R. D. Weisel, M. Radisic and R.-K. Li, *Biomaterials*, 2011, **32**, 1280–1290.
98 J. Bargehr, L. P. Ong, M. Colzani, H. Davaapil, P. Hofsteen, S. Bhandari, L. Gambardella, N. Le Novère, D. Iyer and F. Sampaziotis, *Nat. Biotechnol.*, 2019, **37**, 895–906.
99 M. Lux, B. Andrée, T. Horvath, A. Nosko, D. Manikowski, D. Hilfiker-Kleiner, A. Haverich and A. Hilfiker, *Acta Biomater.*, 2016, **30**, 177–187.
100 K. S. Thomson, F. S. Korte, C. M. Giachelli, B. D. Ratner, M. Regnier and M. Scatena, *Tissue Eng., Part A*, 2013, **19**, 967–977.
101 N. Y. Liaw and W.-H. Zimmermann, *Adv. Drug Delivery Rev.*, 2016, **96**, 156–160.
102 S. R. Shin, C. Zihlmann, M. Akbari, P. Assawes, L. Cheung, K. Zhang, V. Manoharan, Y. S. Zhang, M. Yüksekkaya and K. T. Wan, *Small*, 2016, **12**, 3677–3689.
103 M. Kharaziha, S. R. Shin, M. Nikkhah, S. N. Topkaya, N. Masoumi, N. Annabi, M. R. Dokmeci and A. Khademhosseini, *Biomaterials*, 2014, **35**, 7346–7354.
104 A. Navaei, H. Saini, W. Christenson, R. T. Sullivan, R. Ros and M. Nikkhah, *Acta Biomater.*, 2016, **41**, 133–146.
105 A. Navaei, N. Moore, R. T. Sullivan, D. Truong, R. Q. Migrino and M. Nikkhah, *RSC Adv.*, 2017, **7**, 3302–3312.
106 P. Baei, M. Hosseini, H. Baharvand and S. Pahlavan, *J. Biomed. Mater. Res., Part A*, 2020, **108**(5), 1203–1213.
107 M. C. Barsotti, F. Felice, A. Balbarini and R. Di Stefano, *Biotechnol. Appl. Biochem.*, 2011, **58**, 301–310.
108 Z. Li and J. Guan, *Polymers*, 2011, **3**, 740–761.
109 A. Pal, C. I. Smith, J. Palade, S. Nagaraju, B. A. Alarcon-Benedetto, J. Kilbourne, A. Rawls, J. Wilson-Rawls, B. L. Vernon and M. Nikkhah, *Acta Biomater.*, 2020, **107**, 138–151.
110 D. J. Lee, M. A. Cavasin, A. J. Rocker, D. E. Soranno, X. Meng, R. Shandas and D. Park, *J. Biol. Eng.*, 2019, **13**, 6.
111 K. Nagase, M. Yamato, H. Kanazawa and T. Okano, *Biomaterials*, 2018, **153**, 27–48.
112 A. Navaei, D. Truong, J. Heffernan, J. Cutts, D. Brafman, R. W. Sirianni, B. Vernon and M. Nikkhah, *Acta Biomater.*, 2016, **32**, 10–23.
113 A. Mathur, Z. Ma, P. Loskill, S. Jeeawoody and K. E. Healy, *Adv. Drug Delivery Rev.*, 2016, **96**, 203–213.

 This journal is © The Royal Society of Chemistry 2020

Published on 21 July 2020. Downloaded by ASU Library on 2/2/2021 12:58:01 AM.

114 A. Shapira, R. Feiner and T. Dvir, *Int. Mater. Rev.*, 2016, **61**, 1–19.
115 M. Kitsara, O. Agbulut, D. Kontziampasis, Y. Chen and P. Menasché, *Acta Biomater.*, 2017, **48**, 20–40.
116 M. Kharaziha, M. Nikkhah, S.-R. Shin, N. Annabi, N. Masoumi, A. K. Gaharwar, G. Camci-Unal and A. Khademhosseini, *Biomaterials*, 2013, **34**, 6355–6366.
117 J. M. Holzwarth and P. X. Ma, *J. Mater. Chem.*, 2011, **21**, 10243–10251.
118 J. E. Pomeroy, A. Helfer and N. Bursac, *Biotechnol. Adv.*, 2020, **42**, 107353.
119 J. Zhang, W. Zhu, M. Radisic and G. Vunjak-Novakovic, *Circ. Res.*, 2018, **123**, 244–265.
120 N. T. Feric and M. Radisic, *Stem Cells Transl. Med.*, 2016, **5**, 410–416.
121 J. G. Jacot, J. C. Martin and D. L. Hunt, *J. Biomech.*, 2010, **43**, 93–98.
122 S. Rajabi-Zeleti, S. Jalili-Firoozinezhad, M. Azarnia, F. Khayyatan, S. Vahdat, S. Nikeghbalian, A. Khademhosseini, H. Baharvand and N. Aghdami, *Biomaterials*, 2014, **35**, 970–982.
123 A. van Spreeuwel, N. Bax, A. Bastiaens, J. Foolen, S. Loerakker, M. Borochin, D. Van Der Schaft, C. Chen, F. Baaijens and C. Bouten, *Integr. Biol.*, 2014, **6**, 422–429.
124 X. Zong, H. Bien, C.-Y. Chung, L. Yin, D. Fang, B. S. Hsiao, B. Chu and E. Entcheva, *Biomaterials*, 2005, **26**, 5330–5338.
125 A. Bar and S. Cohen, *Front. Bioeng. Biotechnol.*, 2020, **8**, 126.
126 H. Jawad, N. N. Ali, A. R. Lyon, Q. Z. Chen, S. E. Harding and A. R. Boccaccini, *J. Tissue Eng. Regener. Med.*, 2007, **1**, 327–342.
127 W.-Y. Lee, Y.-H. Chang, Y.-C. Yeh, C.-H. Chen, K. M. Lin, C.-C. Huang, Y. Chang and H.-W. Sung, *Biomaterials*, 2009, **30**, 5505–5513.
128 D. C. Nguyen, T. A. Hookway, Q. Wu, R. Jha, M. K. Preininger, X. Chen, C. A. Easley, P. Spearman, S. R. Deshpande and K. Maher, *Stem Cell Rep.*, 2014, **3**, 260–268.
129 W.-Y. Lee, H.-J. Wei, W.-W. Lin, Y.-C. Yeh, S.-M. Hwang, J.-J. Wang, M.-S. Tsai, Y. Chang and H.-W. Sung, *Biomaterials*, 2011, **32**, 5558–5567.
130 B. R. Desroches, P. Zhang, B.-R. Choi, M. E. King, A. E. Maldonado, W. Li, A. Rago, G. Liu, N. Nath and K. M. Hartmann, *Am. J. Physiol.: Heart Circ. Physiol.*, 2012, **302**, H2031–H2042.
131 T. Y. Kim, C. M. Kofron, M. E. King, A. R. Markes, A. O. Okundaye, Z. Qu, U. Mende and B.-R. Choi, *PLoS One*, 2018, **13**(5), e0196714.
132 M. Y. Emmert, P. Wolint, N. Wickboldt, G. Gemayel, B. Weber, C. E. Brokopp, A. Boni, V. Falk, A. Bosman and M. E. Jaconi, *Biomaterials*, 2013, **34**, 6339–6354.
133 J. Rouwkema, B. F. Koopman, C. A. V. Blitterswijk, W. J. Dhert and J. Malda, *Biotechnol. Genet. Eng. Rev.*, 2009, **26**, 163–178.
134 D. J. Richards, Y. Li, C. M. Kerr, J. Yao, G. C. Beeson, R. C. Coyle, X. Chen, J. Jia, B. Damon and R. Wilson, *Nat. Biomed. Eng.*, 2020, 1–17.
135 M. Radisic, W. Deen, R. Langer and G. Vunjak-Novakovic, *Am. J. Physiol.: Heart Circ. Physiol.*, 2005, **288**, H1278–H1289.
136 R. J. McMurtrey, *Tissue Eng., Part C*, 2016, **22**, 221–249.
137 E. Di Costanzo, A. Giacomello, E. Messina, R. Natalini, G. Pontrelli, F. Rossi, R. Smits and M. Twarogowska, *Math. Med. Biol.*, 2018, **35**, 121–144.
138 Y. Tan, D. Richards, R. C. Coyle, J. Yao, R. Xu, W. Gou, H. Wang, D. R. Menick, B. Tian and Y. Mei, *Acta Biomater.*, 2017, **51**, 495–504.
139 B. M. Ulmer, A. Stoehr, M. L. Schulze, S. Patel, M. Gucek, I. Mannhardt, S. Funcke, E. Murphy, T. Eschenhagen and A. Hansen, *Stem Cell Rep.*, 2018, **10**, 834–847.
140 R. Noguchi, K. Nakayama, M. Itoh, K. Kamohara, K. Furukawa, J.-I. Oyama, K. Node and S. Morita, *J. Heart Lung Transpl.*, 2016, **35**, 137–145.
141 K. Sakaguchi, T. Shimizu and T. Okano, *J. Controlled Release*, 2015, **205**, 83–88.
142 C. K. Griffith, C. Miller, R. C. Sainson, J. W. Calvert, N. L. Jeon, C. C. Hughes and S. C. George, *Tissue Eng.*, 2005, **11**, 257–266.
143 I. Pitaktong, C. Lui, J. Lowenthal, G. Mattson, W.-H. Jung, Y. Bai, E. Yeung, C. S. Ong, Y. Chen and S. Gerecht, *Tissue Eng., Part C*, 2020, **26**, 80–90.
144 P. Beauchamp, C. B. Jackson, L. C. Ozhathil, I. Agarkova, C. L. Galindo, D. B. Sawyer, T. M. Suter and C. Zuppinger, *Front. Mol. Biosci.*, 2020, **7**, 14.
145 C. S. Ong, T. Fukunishi, H. Zhang, C. Y. Huang, A. Nashed, A. Blazeski, D. DiSilvestre, L. Vricella, J. Conte and L. Tung, *Sci. Rep.*, 2017, **7**, 1–11.
146 J. Yang, M. Yamato, C. Kohno, A. Nishimoto, H. Sekine, F. Fukai and T. Okano, *Biomaterials*, 2005, **26**, 6415–6422.
147 S. Sekiya, T. Shimizu, M. Yamato, A. Kikuchi and T. Okano, *Biochem. Biophys. Res. Commun.*, 2006, **341**, 573–582.
148 G. W. Brodland, *J. Biomech. Eng.*, 2002, **124**, 188–197.
149 O. B. Matthys, T. A. Hookway and T. C. McDevitt, *Curr. Stem Cell Rep.*, 2016, **2**, 43–51.
150 S. Halbert, R. Bruderer and T. Lin, *J. Exp. Med.*, 1971, **133**, 677–695.
151 L. Polonchuk, M. Chabria, L. Badi, J.-C. Hoflack, G. Figtree, M. J. Davies and C. Gentile, *Sci. Rep.*, 2017, **7**, 1–12.
152 A. Neto, C. Correia, M. Oliveira, M. Rial-Hermida, C. Alvarez-Lorenzo, R. Reis and J. Mano, *Biomater. Sci.*, 2015, **3**, 581–585.
153 O. Frey, P. M. Misun, D. A. Fluri, J. G. Hengstler and A. Hierlemann, *Nat. Commun.*, 2014, **5**, 1–11.
154 P. Beauchamp, W. Moritz, J. M. Kelm, N. D. Ullrich, I. Agarkova, B. D. Anson, T. M. Suter and C. Zuppinger, *Tissue Eng., Part C*, 2015, **21**, 852–861.
155 S. Breslin and L. O'Driscoll, *Drug Discovery Today*, 2013, **18**, 240–249.
156 A. P. Napolitano, D. M. Dean, A. J. Man, J. Youssef, D. N. Ho, A. P. Rago, M. P. Lech and J. R. Morgan, *Biotechniques*, 2007, **43**, 494–500.
157 J. M. Cha, H. Park, E. K. Shin, J. H. Sung, O. Kim, W. Jung, O. Y. Bang and J. Kim, *Biofabrication*, 2017, **9**, 035006.
158 E. Fennema, N. Rivron, J. Rouwkema, C. van Blitterswijk and J. de Boer, *Trends Biotechnol.*, 2013, **31**, 108–115.
159 J. Dahlmann, G. Kensah, H. Kempf, D. Skvorc, A. Gawol, D. A. Elliott, G. Dräger, R. Zweigerdt, U. Martin and I. Gruh, *Biomaterials*, 2013, **34**, 2463–2471.

Published on 21 July 2020. Downloaded by ASU Library on 2/2/2021 12:58:01 AM.

160 E. Giacomelli, M. Bellin, L. Sala, B. J. Van Meer, L. G. Tertoolen, V. V. Orlova and C. L. Mummery, *Development*, 2017, **144**, 1008–1017.
161 E. Giacomelli, V. Meraviglia, G. Campostrini, A. Cochrane, X. Cao, R. W. van Helden, A. K. Garcia, M. Mircea, S. Kostidis and R. P. Davis, *Cell Stem Cell*, 2020, **26**(6), 862–879.e11.
162 S. M. Ravenscroft, A. Pointon, A. W. Williams, M. J. Cross and J. E. Sidaway, *Toxicol. Sci*, 2016, **152**, 99–112.
163 T. Shimizu, M. Yamato, Y. Isoi, T. Akutsu, T. Setomaru, K. Abe, A. Kikuchi, M. Umezu and T. Okano, *Circ. Res.*, 2002, **90**, e40–e48.
164 S. Masuda and T. Shimizu, *Adv. Drug Delivery Rev.*, 2016, **96**, 103–109.
165 D. Chang, T. Shimizu, Y. Haraguchi, S. Gao, K. Sakaguchi, M. Umezu, M. Yamato, Z. Liu and T. Okano, *PLoS One*, 2015, **10**(10), e0137494.
166 H. Masumoto, T. Ikuno, M. Takeda, H. Fukushima, A. Marui, S. Katayama, T. Shimizu, T. Ikeda, T. Okano and R. Sakata, *Sci. Rep.*, 2014, **4**, 6716.
167 J. A. Davies, in *Organoids and Mini-Organs*, ed. J. A. Davies and M. L. Lawrence, Academic Press, 2018, pp. 3–23.
168 D. J. Richards, R. C. Coyle, Y. Tan, J. Jia, K. Wong, K. Toomer, D. R. Menick and Y. Mei, *Biomaterials*, 2017, **142**, 112–123.
169 X. Lian, J. Zhang, S. M. Azarin, K. Zhu, L. B. Hazeltine, X. Bao, C. Hsiao, T. J. Kamp and S. P. Palecek, *Nat. Protoc.*, 2013, **8**, 162.
170 Y. Yan, J. Bejoy, J. Xia, K. Griffin, J. Guan and Y. Li, *Sci. Rep.*, 2019, **9**, 1–12.
171 Z. Ma, J. Wang, P. Loskill, N. Huebsch, S. Koo, F. L. Svedlund, N. C. Marks, E. W. Hua, C. P. Grigoropoulos and B. R. Conklin, *Nat. Commun.*, 2015, **6**, 1–10.
172 F. Oltolina, A. Zamperone, D. Colangelo, L. Gregoletto, S. Reano, S. Pietronave, S. Merlin, M. Talmon, E. Novelli and M. Diena, *PLoS One*, 2015, **10**(9), e0137999.
173 S. Rungarunlert, N. Klincumhom, I. Bock, C. Nemes, M. Techakumphu, M. K. Pirity and A. Dinnyes, *Biotechnol. Lett.*, 2011, **33**, 1565–1573.
174 S. Zhao, Z. Xu, H. Wang, B. E. Reese, L. V. Gushchina, M. Jiang, P. Agarwal, J. Xu, M. Zhang and R. Shen, *Nat. Commun.*, 2016, **7**, 1–12.
175 S. Niebruegge, C. L. Bauwens, R. Peerani, N. Thavandiran, S. Masse, E. Sevaptisidis, K. Nanthakumar, K. Woodhouse, M. Husain and E. Kumacheva, *Biotechnol. Bioeng.*, 2009, **102**, 493–507.
176 M. Kharaziha, A. Memic, M. Akbari, D. A. Brafman and M. Nikkhah, *Adv. Healthcare Mater.*, 2016, **5**, 1533–1553.
177 D. Chimene, D. L. Alge and A. K. Gaharwar, *Adv. Mater.*, 2015, **27**, 7261–7284.
178 R. Amezcua, A. Shirolkar, C. Fraze and D. A. Stout, *Nanomaterials*, 2016, **6**, 133.
179 S. R. Shin, S. M. Jung, M. Zalabany, K. Kim, P. Zorlutuna, S. B. Kim, M. Nikkhah, M. Khabiry, M. Azize and J. Kong, *ACS Nano*, 2013, **7**, 2369–2380.
180 A. Paul, A. Hasan, H. A. Kindi, A. K. Gaharwar, V. T. Rao, M. Nikkhah, S. R. Shin, D. Krafft, M. R. Dokmeci and D. Shum-Tim, *ACS Nano*, 2014, **8**, 8050–8062.
181 M. Mehrali, A. Thakur, C. P. Pennisi, S. Talebian, A. Arpanaei, M. Nikkhah and A. Dolatshahi-Pirouz, *Adv. Mater.*, 2017, **29**, 1603612.
182 A. Navaei, K. R. Eliato, R. Ros, R. Q. Migrino, B. C. Willis and M. Nikkhah, *Biomater. Sci.*, 2019, **7**, 585–595.
183 L. Karperien, A. Navaei, B. Godau, A. Dolatshahi-Pirouz, M. Akbari and M. Nikkhah, *Nanoengineered Biomaterials for Regenerative Medicine*, Elsevier, 2019, pp. 95–124.
184 R. K. Kankala, K. Zhu, X.-N. Sun, C.-G. Liu, S.-B. Wang and A.-Z. Chen, *ACS Biomater. Sci. Eng.*, 2018, **4**, 800–818.
185 E. E. Connor, J. Mwamuka, A. Gole, C. J. Murphy and M. D. Wyatt, *Small*, 2005, **1**, 325–327.
186 N. Khlebtsov and L. Dykman, *Chem. Soc. Rev.*, 2011, **40**, 1647–1671.
187 R. Shukla, V. Bansal, M. Chaudhary, A. Basu, R. R. Bhonde and M. Sastry, *Langmuir*, 2005, **21**, 10644–10654.
188 A. M. Alkilany and C. J. Murphy, *J. Nanopart. Res.*, 2010, **12**, 2313–2333.
189 G. Frens, *Nat. Phys. Sci.*, 1973, **241**, 20–22.
190 L. Dykman and N. Khlebtsov, *Chem. Soc. Rev.*, 2012, **41**, 2256–2282.
191 K. Ashtari, H. Nazari, H. Ko, P. Tebon, M. Akhshik, M. Akbari, S. N. Alhosseini, M. Mozafari, B. Mehravi and M. Soleimani, *Adv. Drug Delivery Rev.*, 2019, **144**, 162–179.
192 S. T. Holgate, *J. Biomed. Nanotechnol.*, 2010, **6**, 1–19.
193 F.-Q. Nie, Z.-K. Xu, X.-J. Huang, P. Ye and J. Wu, *Langmuir*, 2003, **19**, 9889–9895.
194 L. Sun, C. Huang, T. Gong and S. Zhou, *Mater. Sci. Eng., C*, 2010, **30**, 583–589.
195 M. Xu, J. Zhu, F. Wang, Y. Xiong, Y. Wu, Q. Wang, J. Weng, Z. Zhang, W. Chen and S. Liu, *ACS Nano*, 2016, **10**, 3267–3281.
196 Y. Tan, D. Richards, R. Xu, S. Stewart-Clark, S. K. Mani, T. K. Borg, D. R. Menick, B. Tian and Y. Mei, *Nano Lett.*, 2015, **15**, 2765–2772.
197 D. J. Richards, Y. Tan, R. Coyle, Y. Li, R. Xu, N. Yeung, A. Parker, D. R. Menick, B. Tian and Y. Mei, *Nano Lett.*, 2016, **16**, 4670–4678.
198 J. Park, Y. S. Kim, S. Ryu, W. S. Kang, S. Park, J. Han, H. C. Jeong, B. H. Hong, Y. Ahn and B. S. Kim, *Adv. Funct. Mater.*, 2015, **25**, 2590–2600.
199 S. Ahadian, Y. Zhou, S. Yamada, M. Estili, X. Liang, K. Nakajima, H. Shiku and T. Matsue, *Nanoscale*, 2016, **8**, 7075–7084.
200 P. Hoang, J. Wang, B. R. Conklin, K. E. Healy and Z. Ma, *Nat. Protoc.*, 2018, **13**, 723.
201 K. A. Gerbin, X. Yang, C. E. Murry and K. L. Coulombe, *PLoS One*, 2015, **10**(7), e0131446.
202 M. Y. Emmert, P. Wolint, S. Winklhofer, P. Stolzmann, N. Cesarovic, T. Fleischmann, T. D. Nguyen, T. Frauenfelder, R. Böni and J. Scherman, *Biomaterials*, 2013, **34**, 2428–2441.
203 A. Kermanizadeh, D. Balharry, H. Wallin, S. Loft and P. Møller, *Crit. Rev. Toxicol.*, 2015, **45**, 837–872.
204 A. Kawamura, S. Miyagawa, S. Fukushima, T. Kawamura, N. Kashiyama, E. Ito, T. Watabe, S. Masuda, K. Toda and J. Hatazawa, *Sci. Rep.*, 2016, **6**, 19464.

 This journal is © The Royal Society of Chemistry 2020